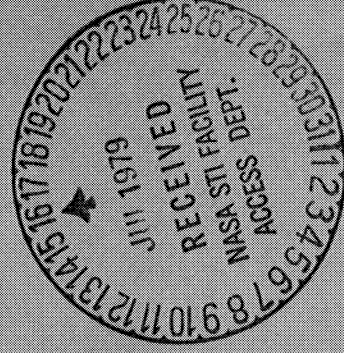


NASA Technical Memorandum X-71763

Interim Prediction Method for Fan and Compressor Source Noise

Marcus F. Heidmann

JUNE 1979



The NASA logo, consisting of the word "NASA" in a bold, italicized, sans-serif font.

First printing, 1975.

NASA Technical Memorandum X-71763

Interim Prediction Method for Fan and Compressor Source Noise

Marcus F. Heidmann
Lewis Research Center
Cleveland, Ohio

NASA

National Aeronautics
and Space Administration

**Scientific and Technical
Information Branch**

1979

SUMMARY

A prediction method is presented for interim use by NASA for evaluating and assessing the noise generated by fans and compressors of turbojet and turbofan aircraft engines. The method was formulated in partial support of the NASA Aircraft Noise Prediction Program (ANOPP). Spectral distributions of the sound pressure levels referenced to 20 micronewtons per square meter at a 1-meter radius in a free field are predicted as a function of the polar angle about the fan or compressor axis. The total noise levels are obtained by spectrally summing the predicted levels of broadband, discrete-tone, and combination-tone noise components.

The interim prediction method is a modification of a method previously developed by other investigators. The modifications are based on a partial analysis of data from full-scale, single-stage fan tests performed at NASA Lewis Research Center. A discussion of the modifications and a detailed procedure for the prediction are presented. Comparisons of the predicted and measured noise of the NASA fans are presented and discussed. Some major problem areas and research requirements are identified.

INTRODUCTION

NASA is engaged in a variety of programs directed toward reducing the noise associated with aircraft operation. A significant source of the noise produced by aircraft is that generated by fans and compressors for aircraft engines. Both contractual and in-house studies are being supported by NASA to explore and develop quieter fans and compressors for a variety of engine cycles and types of aircraft. One requirement frequently arising from such studies is the ability to readily establish and assess the noise performance of fans and compressors. The source noise of new or existing fan-compressor designs or applications must often be evaluated relative to previous experience, the specification of acoustic treatment, and the impact on community noise levels. What is needed is a specific and comprehensive method of predicting the source noise of any fan or compressor to a quantitative precision which reflects the state-of-the-art. NASA's objective is to develop and continuously update such a prediction method. There is an immediate need, however, to specify a prediction method which can be used until comprehensive prediction methods can be fully explored, developed, and verified. The purpose of this report is to specify an interim prediction

method for fan and compressor source noise in terms of its free-field spectral and directivity properties.

An interim prediction method is specified in response to the immediate need for predicting fan-compressor noise as a component of the total aircraft noise for the NASA Aircraft Noise Prediction Program (ANOPP). This NASA Langley Research Center program is being developed jointly by various NASA centers with help from industry representatives. The purpose of ANOPP is to develop a comprehensive method of predicting noise footprints for single or multiple event air-flights which reflects the state-of-the-art and is useful in exploring technological advances to economically reduce community noise levels.

This report first discusses the approach used to formulate the interim prediction method and the scope of this study with regard to the applicable literature. The method is then introduced by a general description of the prediction procedure where the applications and the necessary design and operating parameters of a fan or compressor are also specified. The noise properties of fans and compressors used in the prediction method are then specified within a limited framework of background material. A specific procedure for predicting free-field noise patterns follows. Finally, comparisons of measured and predicted results are made, and some remarks are presented about problem areas and future research requirements.

SYMBOLS

B	number of rotor blades
$F_1, F_2, \text{etc.}$	functions as given by appropriate curves
f	frequency, Hz
f_b	blade passage frequency, $B\Omega$, Hz
L	sound pressure level correction, dB (referenced to $20 \mu\text{N}/\text{m}^2$ at 1-m radius)
L_c	characteristic sound pressure level, dB (referenced to $20 \mu\text{N}/\text{m}^2$ at 1-m radius)
L_n	normalized peak noise level, dB (referenced to $20 \mu\text{N}/\text{m}^2$ at 1-m radius)
M_T	rotor tip or wheel speed Mach number
M_{TR}	rotor tip relative inlet Mach number
$(M_{TR})_D$	M_{TR} at fan design point

\dot{m}	mass flow rate passing through fan or compressor
\dot{m}_0	reference value of \dot{m} (0.453 kg/sec, 1 lbm/sec)
PNL	perceived noise level, dB
PR	fan stage total pressure ratio
PWL	sound power level, dB (referenced to 10^{-13} W)
RSS	rotor-stator spacing factor (see fig. 14(a))
SHP	rotor shaft horsepower
SPL(f)	spectrum level as function of frequency, dB
T	total temperature at fan face, K ($^{\circ}$ R)
ΔT	total temperature rise across a fan or compressor stage, $\Delta T/T =$ $\left[(\text{PR})^{(\gamma-1)/\gamma} - 1 \right] / \eta_c$
ΔT_0	reference value of ΔT (0.555 K, 1° R)
V	number of stator blades
δ	cutoff factor (see eq. (3))
η_c	fan stage adiabatic efficiency
θ	directivity or polar angle reference to inlet axis
Ω	wheel speed, rev/sec

APPROACH AND SCOPE

The approach used herein to formulate an interim prediction method was to modify an existing method. The prediction method adopted for this purpose was the fan and compressor portion of a more comprehensive prediction program recently developed by the Boeing Company under contract with the NASA Ames Research Center. This prediction method is explicitly specified in reference 1. The modifications to the Boeing-Ames prediction method made at this time are entirely related to correlations and interpretations of the acoustic data from the full-scale fan tests performed at NASA Lewis (reported in refs. 2 to 4). Some of the prediction curves and equations specified in the interim prediction method correspond exactly to those appearing in the Boeing-Ames method. In particular, the extension of single-stage fan prediction to multistage fans and compressors is used as specified.

The Boeing-Ames method was selected for modification because it is a thoroughly documented method and is addressed to the total problem of providing far-field directivity and spectral properties from multiple sources, features considered essential for the interim prediction method. The choice of the method was from among a variety of empirically and theoretically based prediction methods. Most of these other methods do not provide complete far-field properties or are restricted to a single noise source or noise component. For example, the frequently referenced correlation of Smith and House (ref. 5) does not provide far-field directivity. Only two well-documented prediction methods in addition to the Boeing-Ames method appeared to satisfy the needs of this study. Although these methods (refs. 6 and 7) were formulated at an earlier date, they prescribe prediction procedures in many ways similar to the Boeing-Ames method. The Boeing-Ames method was adopted because it used a data base acquired from operational aircraft rather than from scale model static tests and because it more nearly satisfied the immediate needs of NASA. Some additional prediction methods developed by the aeronautics industries which may satisfy the needs of NASA are referred to in the literature (refs. 8 to 11). Many of the details of these methods, however, have not been disclosed.

A survey and evaluation of the reported prediction methods and techniques are beyond the intended scope of this study. In this regard, it should be pointed out that no reported prediction method has received a comprehensive evaluation against available data. In general, these methods have been examined only for the manner in which they fit the data base from which they were obtained. Another purpose of the interim prediction method is that it is a vehicle by which models and techniques of other prediction methods can be evaluated. Such evaluations are considered to be best accomplished within the matrix of a multiple source - multiple component prediction method rather than by examining the isolated behavior of a specific source or component.

The main objective of this study is to provide a precise and all-encompassing prediction method which assimilates all the available technology. The currently used prediction methods are basically empirical with only a phenomenological application of theory. A more quantitative application of theoretical analysis appears necessary for precise and all-encompassing predictions. The theoretical literature on noise generation by turbomachinery is extensive and growing. A review of this literature and potential applications to the prediction method are not covered in this initial study.

One aspect of the theoretical literature may be particularly significant with regard to upgrading the prediction method. This involves the coupling between a noise source and its far-field noise pattern. The theoretical coupling between a fan or compressor noise source and the far-field noise pattern involves wave propagation through ducts and duct terminations so that the free-field pattern depends on both the source and the duct properties. From an ideal theoretical standpoint, the source noise should be

characterized by the amplitudes of the propagating modes entering the duct rather than by the far-field noise patterns as currently used in prediction methods. A major problem in this regard is that the specification of the propagating modes depends on exact descriptions of the complex unsteady flow patterns within a fan or compressor. Unfortunately, substantiated techniques which relate free-field problems to modal amplitudes for operational fans do not now exist. However, their development could significantly affect the method for predicting the source noise or the approach to any upgrading effort as now envisioned.

GENERAL DESCRIPTION OF PREDICTION METHOD

An interim procedure for predicting the source noise for fan and compressor stages was formulated based on the Boeing-Ames method described in reference 1. The procedure predicts the one-third octave band spectral intensities of the free-field noise pattern. The noise is assumed to be propagating from a "virtual source" at a point defined by the plane and axis of a fan compressor. The intensities are given as the sound pressure levels (in dB referenced to $20 \mu\text{N}/\text{m}^2$) at a 1-meter radius and are devoid of any atmospheric attenuation or ground effects. The predicted free-field radiation varies with the polar angle about the fan or compressor axis and is assumed to be symmetric about this axis. The prediction method is applicable to turbojet compressors and to single- and two-stage turbofans with and without inlet guide vanes. The fans or compressors are assumed to be representative of good aerodynamic design with the operating point near the normal operating line and not above the design point. It is assumed that the inlet and discharge duct configurations are such that they neither cause nor attenuate the generated noise - that is, short ducts with no blow-in doors, aerodynamically poor obstructions, or acoustic treatment.

The predicted free-field radiation patterns consist of a composite of the following separately predicted noise components:

- (1) Noise emitted from the fan or compressor inlet duct
 - (a) Broadband noise
 - (b) Discrete-tone noise
 - (c) Combination-tone noise
- (2) Noise emitted from the fan discharge duct
 - (a) Broadband noise
 - (b) Discrete-tone noise

The procedure involves predicting the spectrum shape, spectrum level, and free-field directivity for each of the noise components. The component spectra at any polar angle are then combined on an energy basis to form a single spectrum. The procedure

is specifically directed toward a single-stage fan. For two-stage fans, each stage is treated as an independent source and the sound energy produced by each stage is combined. No correction is made for blade row attenuation. In the case of a turbojet engine, the noise from the first compressor stage is assumed to be representative of the far-field noise. These multistage fan and compressor procedures are those of the Boeing-Ames method and are not reexamined in this study.

The spectrum shape of each component is basically fixed, and the spectral predictions primarily involve positioning the spectrum shape within the frequency domain. This positioning is accomplished in all cases by referencing the spectral frequencies to the blade passage tone frequency. The blade passage tone frequency, therefore, is one of the basic parameters required in the prediction procedure.

Predictions of the spectrum levels of each of the components depend on the design and performance parameters of the fans and compressors. A spectrum level is predicted for a reference polar angle and the complete far-field pattern is obtained from specified directivity corrections. Each component, therefore, is characterized by a fixed spectral distribution which varies in level with the polar angle. Since the directivity corrections differ for each noise component, they give the result of a varying spectra as well as level with polar angle when they are combined.

Four parameters must be specified to predict the basic spectrum levels: the mass flow rate and total temperature rise associated with a fan or compressor stage and the design and operating point values of the rotor tip relative inlet Mach number. These basic levels are then corrected or adjusted. One correction depends on the presence or absence of inlet guide vanes. Such vanes are always present for the second stage of a conventional two-stage fan. A correction is also applied for rotor-stator spacing effects. For a rotor with both inlet and exit stators the correction depends solely on the most closely spaced stator.

Two additional corrections are applied to the spectrum levels or shapes. One concerns inlet flow distortions and the other tone cutoff. A qualitative identification of inlet flow distortions or irregularities must be made and corrections are applied for these distortions independent of their severity. At this time it is recommended that the correction be applied for all static and ground roll operating conditions and neglected for flight conditions unless there are compelling reasons to assume otherwise.

The corrections for tone cutoff are based on the studies of Tyler and Sofrin (ref. 12). The criterion for cutoff requires the specification of the number of rotor and stator blades and the rotor tip Mach number. A simplified form of the cutoff criterion is used where the fundamental tone alone is suppressed with cutoff.

The next section discusses and describes the noise properties that will be used in the explicit prediction procedure presented later in this report. In particular, modifications based on the NASA Lewis data of the noise properties used in the Boeing-Ames

method are discussed. Both the original and modified curves and criteria needed for the prediction procedure are presented.

CHARACTERIZATION OF NOISE PROPERTIES

General Properties

The Boeing-Ames method essentially involves a procedure wherein corrections are applied to normalized values of sound pressure levels for each component noise source. The normalization accounts for large differences in the design and performance of a fan or compressor stage and the corrections account for differences in design detail. The normalization parameters used, or at least inferred, in the Boeing-Ames method are the fan stage total pressure rise and either the fan diameter or the exhaust duct area. These normalization parameters were modified or changed for the interim prediction method.

The changes in normalization parameters were based on the noise correlations for full-scale fans (table I) tested at NASA Lewis and reported in reference 3. In this study it was assumed that a fan is a noise generator in which a certain fraction of the input mechanical power is converted to output sound power. An examination of the data showed that the conversion is strongly related to the specific work performed on the air during the compression process. This specific work is proportional to ΔT , the total temperature rise incurred during compression. Figure 1 shows the correlation for total sound power levels from reference 3. Mechanical power and specific work proved to be good correlating parameters for all fans having similar noise sources. Fan C in figure 1 is an exception because it has an additional noise source (combination tone noise) caused by supersonic tip speed operation. On the basis of this correlation the mechanical power and specific work were used to formulate the normalization parameters.

For the convenience of specifying commonly used fan or compressor variables, the equivalent of power and specific work are used to normalize the levels of all the component noise sources. The product of mass flow rate \dot{m} and temperature rise ΔT is used for power. Specific work is expressed as temperature rise. Using these equivalents gives the general form of the normalized sound pressure levels as

$$\text{SPL} - 20 \log_{10} \left(\frac{\Delta T}{\Delta T_0} \right) - 10 \log_{10} \left(\frac{\dot{m}}{\dot{m}_0} \right) = f(\text{design detail}) \quad (1)$$

In reality, the ultimate precision of an empirical prediction method does not depend on the selection of the normalizing parameters. The parameters selected, however, can

affect the complexity of the corrections needed to attain precision. The reason for selecting power and specific work is that they are considered more encompassing in describing a fan with regard to noise generation than are pressure rise and a duct dimension as used in the Boeing-Ames method.

Although power and specific work appear to normalize the NASA Lewis data, there is evidence of a residual effect of rotor tip relative inlet Mach number. This is shown in figure 2 where normalized values of sound power level are shown as functions of this relative Mach number. At or near a tip relative inlet Mach number of 1.0, the noise levels appear to peak and then decrease with increasing Mach number. As a result of this general behavior the normalized levels of all the component noise sources will be adjusted for the effects of rotor tip relative inlet Mach number M_{TR} . With the exception of predicting combination tone noise, adjustments or correlations for M_{TR} were not used in the Boeing-Ames method. In addition to the operating value of the Mach number M_{TR} , the design value of rotor tip relative inlet Mach number $(M_{TR})_D$ is used to adjust the normalized levels. This effect is generally masked in figure 2 because the levels have not been corrected for other variables which affect noise generation. Fan C, however, shows a high noise level for its high value of $(M_{TR})_D$.

Broadband Noise

The prediction of broadband noise by this interim method is directed toward predicting the average behavior of the apparent broadband noise underlying the tones in a one-third octave display of the fan noise. At one time vortex shedding from blade and vanes was considered to be the major source of broadband noise in fans and compressors. More recently, broadband noise, whether generated by fluctuating-lift dipole sources or by quadropole sources, is generally associated with random unsteadiness or turbulence in the flow passing the blading. Among the possible sources of randomly unsteady flow are turbulence in the wall and blade boundary layers, in the blade wakes and vortices, or in the freestream inlet flow.

Broadband noise may also be attributed to the modulation of a tone generating mechanism. Both frequency and phase modulation of tones caused by nonrepeating wakes behind blade rows will be partially resolved spectrally as a continuum. Considering the many potential sources of broadband noise, prediction on the basis of individual sources is beyond the scope of the interim prediction method.

In the quantitative description of the broadband noise component properties that follows, the description format corresponds to that used in the Boeing-Ames method. The description consists of the spectrum content, spectrum level, level corrections for particular design and operating conditions, and, finally, the directivity correction

needed to predict the free-field radiation pattern. This format will also be used for the discrete and combination tone components. The component properties are presented for subsequent use in the prediction procedure.

Spectrum content. - An analytical expression for the spectrum content of the apparent broadband noise for the Lewis fan test data was derived from one-third octave band spectral analysis (ref. 3). The solid curve in figure 3(a) shows this broadband noise spectrum. It is characterized by a log normal distribution function with a center frequency of $2\frac{1}{2}$ times the blade passage frequency f_b . This spectrum shape, shown in figure 3(a), is given by

$$L = 10 \log_{10} e^{-1/2} \left[\frac{\ln \left(\frac{f}{2.5 f_b} \right)}{\ln \sigma} \right]^2 \quad (2)$$

where σ (geometric mean deviation) is equal to 2.2.

The spectrum content provided in the Boeing-Ames method (ref. 1) is shown by the dashed curve in figure 3(a). But figure 3(a) does not give a true comparison of the differences in spectra. While the Boeing-Ames method prescribes the content at a 45.7-meter (150-ft) radial distance from the fan and hence includes the distorting effect of atmospheric attenuation, the log normal distribution describes the source spectrum without this effect. Correcting the Boeing-Ames spectrum by removing atmospheric attenuation would reduce the difference at high frequencies.

Caution should be exercised when using the predicted spectrum shape given by equation (2). Many fans exhibit considerably more spectral detail than is represented by the simplification used in figure 3(a). For example, as depicted in figure 3(b), several of the Lewis fans show evidence of bimodal spectral properties with another lower level log normal distribution centered at a higher frequency (ref. 3). Since this secondary mode was not adequately defined by the data, it could not be used for prediction purposes and is therefore neglected at this time. Theoretically, the broadband spectrum shape may be expected to be composed of a number of spectral modes depending on the number of sources. The spectral properties of the stronger sources should suffice as a source description for unsuppressed fans, but weaker sources could be important after transmission through soft-wall ducts. There is no guarantee that acoustic suppressions will provide equal attenuation for all broadband sources at a given frequency.

Spectrum level. - In the prediction procedure, the broadband noise radiating upstream out of the inlet and that radiating downstream out of the fan discharge nozzle

are separately predicted. The spectrum levels of these inlet and discharge components at the polar angles for peak radiation are predicted to vary as shown in figure 4. The normalized level is shown to vary with both the design point and operating point values of the rotor tip relative inlet Mach number. These curves are based on an analysis of the Lewis fan test data. They differ from that specified by the Boeing-Ames method as approximately shown by the dashed lines. An exact comparison in figure 4 is not possible because fan diameter and discharge nozzle area were used as scaling parameters in the Boeing-Ames method. Hence, it was necessary to use approximations based on typical fan design in order to establish the Boeing-Ames broadband prediction curve in figure 4. The principal difference in the predictions methods concerns a dependence of the noise on both the design and operating point values of the relative inlet Mach number. The recommended curves, in effect, predict a higher noise level for a given fan operating at part speed compared to the same fan operating at design speed.

The prediction curves in figure 4 are based on the broadband noise characteristics of the Lewis full-scale fan data shown in figure 5. The sound power level of the broadband noise decreased when the tip relative inlet Mach number exceeded a value near 1.0 (as in the case of total power in fig. 2). The average effect of the design point Mach number $(M_{TR})_D$ shown in figure 5 was used to formulate figure 4. Separation of the inlet and discharge components of the broadband noise has not been completed, but a partial analysis shows that both components decrease at high Mach numbers and have comparable overall levels. It was noted, however, that the inlet component exhibited a decrease in level when the Mach number exceeded a value somewhat less than 1.0. These results are reflected in the curves of figure 4.

Inlet-guide-vane correction. - The correction for inlet guide vanes specified in the Boeing-Ames method is applied to the broadband noise levels given by figure 4. For fan stages with inlet guide vanes or a preceding fan stage, the level for the discharge duct is increased by 3 decibels.

Rotor-stator spacing correction. - The correction for rotor-stator spacing specified in the Boeing-Ames method is also applied to the broadband levels given by figure 4. The correction is based on the spacing factor RSS defined in figure 6(a). The level correction is given by $\Delta \text{ dB} = -5 \log RSS/300$ and shown by the solid line in figure 6(b). The spacing corrections are applied to both inlet and discharge duct broadband components.

Inlet flow distortion adjustment. - The static fan tests performed at NASA Lewis did not show a strong effect of rotor-stator spacing on broadband noise levels. The insensitivity to spacing is attributed to the dominance of broadband noise generated by inlet flow distortions over that caused by rotor-stator interactions. This distortion-

related noise is an additional broadband source that is insensitive to variations in rotor-stator spacing.

Ideally, both distortion and interaction-related noise sources should be calculated separately and added on an energy basis in predicting the total broadband noise level. A quantitative description of the distortion-related noise is not attempted at this time, and the following interim procedure is recommended for predicting broadband levels for static and ground roll operation. The rotor-stator spacing factor RSS is arbitrarily assigned a value of 100 unless in reality it is less than this value. The adjustment is shown by the dashed line in figure 6(b). In effect, this procedure implies that interaction related noise will dominate the broadband noise only when the rotor-stator spacing factor is less than 100.

Although the modification of the Boeing-Ames method for distortion effects is primarily specified to provide better agreement between the predicted and measured noise for NASA Lewis fans, it is expected to be generally applicable to static and ground roll operating conditions where inlet flow distortions are present.

Directivity correction. - The average directivities of the broadband noise from the inlet and discharge ducts as observed in the NASA fan data are shown in figure 7. The directivities as functions of polar angle are given as corrections for the peak spectrum level specified in figure 4. Also shown in figure 7 are the directivities specified by the Boeing-Ames method. Differences in the two directivities are largely confined to polar angles near 90° and the overlap region of inlet and discharge quadrants.

Discrete Tone Noise

Discrete tones at integer multiples of the fundamental blade passage frequency are radiated from fans and compressors when operated at either subsonic or supersonic tip speeds. Discrete tone generation is generally associated with lift fluctuations on rotor or stator blades. The lift fluctuations originate from a variety of sources. The wakes trailing behind inlet guide vanes and behind rotor blades are the most prominent sources of the fluctuations. The lift fluctuations are related to the static pressure field generated when either the rotor chops a wake or the rotating wakes impinge on a stator blade. Tones generated in this manner are referred to as interaction tones.

Inlet flow turbulence is another source of lift fluctuations that generates discrete tones when its scale is large. Inlet flow distortion can also be a major source of discrete tone noise. The tones observed in static tests of fans are suspected to arise from inlet flow distortions. The distortions are attributed to both the proximity of flow-diverting obstacles in the vicinity of the test stand and to the ingestion of packets of free air turbulence or vorticity.

The tones generated by interactions between rotors and stators with unequal number of blades are usually thought to propagate as spinning duct modes, whereas tones caused by equal number of blades and by inlet flow distortions can propagate as either spinning or plane waves. The far-field noise pattern depends on the modal structure of the wave system at the duct exit. It is not possible at this time to extract the exact contributions of the various duct modes or to identify the sources of the modes from far-field fan noise data. The prediction method, therefore, is confined to the average properties observed in tone noise.

The properties of the discrete tone noise that will be used in the prediction procedure are described in the following paragraphs.

Spectrum content. - The spectrum for the discrete tones consists of the first ($k = 1$) and higher ($k > 1$) harmonic orders of the blade passage tones where the first harmonic is at the fundamental blade passage frequency f_b . The spectrum content to be described is the relative noise levels of these tone harmonics. In all cases the harmonic noise level L is referenced to a characteristic or basic noise level L_c which will be established from subsequent spectrum level curves. Two sources of discrete tone noise are described. One consists of the tones normally associated with rotor-stator flow interactions. The other source is attributed to inlet flow distortions. Harmonic levels of the rotor-stator interaction tones are described first.

Spectrum content of the rotor-stator interaction tones depends on the presence of inlet guide vanes and the value of a tone cutoff factor δ . If the cutoff factor is neglected momentarily, the harmonic level L for fan stages without inlet guide vanes for any harmonic order k is given by $L = 3 - 3k$. With inlet guide vanes the harmonic level is given by $L = 0$ for $k = 1$ and $L = -3 - 3k$ for $k \geq 2$. These relative levels of the tone harmonics are illustrated in figure 8. Also shown in figure 8 is a correction based on the cutoff factor δ .

A simplified form of the cutoff factor δ for the fundamental tone is

$$\delta = \left| \frac{M_T}{1 - \frac{V}{B}} \right| \quad (3)$$

where V and B are the number of stator and rotor blades, respectively, and M_T is the rotor tip or wheel speed Mach number. An evaluation is needed to determine whether the cutoff factor is less than or greater than the critical value of 1.05. If the value is less than or equal to 1.05, the fundamental tone level is reduced by 8 decibels as illustrated in figure 8. The correction is not used when M_T exceeds 1.05.

Except for the correction for tone cutoff, the spectrum content shown in figure 8 is that specified in the Boeing-Ames method. A qualitative interpretation of the NASA

Lewis data appears to agree with that data shown in figure 8(a) for fan stages without inlet guide vanes. Experiments have not been performed at Lewis to substantiate the behavior data shown in figure 8(b) for fan stages with inlet guide vanes.

The spectrum correction for cutoff is an attempt to account for its gross effects. Incorporating the correction in the prediction method is based on theoretical considerations and on interpretations of the NASA Lewis fan data. In reality, cutoff calculations are not only more complex than those specified by equation (3), but they also involve a degree of effectiveness. These additional complexities are neglected at this time because they have not been quantitatively established in fan tests.

The harmonic level for the tones attributed to inlet flow distortions is assumed to be given by $L = 10 - 10k$ as shown in figure 9. The NASA Lewis data imply a very rapid falloff in harmonic noise level with increasing harmonic order for the distortion tones compared to that for rotor-stator interaction tones (10 dB/harmonic compared to 3 dB/harmonic). The data also imply that the basic noise level L_c for the distortion tones is equal to that for the rotor-stator interaction tones. At this time, the basic noise levels L_c for both tone sources are assumed to be identical and are established from the same spectrum level curves that will be presented.

As previously recommended, inlet flow distortions should be assumed to be present for all static and ground roll operating conditions. The prediction of distortion-related tones is confined to the inlet duct. With flow distortions two-tone spectra for the inlet duct are predicted - one for rotor-stator tones and another for distortion tones. These two spectra are added on an energy basis to provide a single spectra. The directivity correction to be specified later is applicable to this combined spectra. This combined treatment is used because the individual directivities of the two tone sources have not been identified in the data.

Spectrum level. - The normalized peak levels for the tones are given in figure 10. Separate prediction curves are specified for the tones radiating from the inlet and exhaust ducts. The normalized level of the tones is shown to be a function of both the design and operating values of the tip relative inlet Mach number as was the case for broadband noise levels. The form of the curves for the discharge noise is identical to that for broadband noise. The inlet noise level curves, however, exhibit a substantial peak near a Mach number of 1.0. Also shown in figure 10 are the levels specified in the Boeing-Ames method when approximate parameter relationships for typical fans are used.

The tone levels shown in figure 10 are based on test data from the NASA Lewis fans. The total power content (inlet plus discharge levels) of the tones from the Lewis tests (ref. 3) is shown in figure 11. The normalized level of the tonal power exhibits the peaking behavior near a Mach number of 1.0. A more detailed examination of the data showed this peaking behavior to be most prominent in the noise propagating from

the inlet duct. The behavior for the inlet noise specified in figure 10 was actually constructed from several iterations of using the results from the prediction procedure described herein to match the experimental results.

Inlet-guide-vane correction. - The correction for inlet guide vanes specified in the Boeing-Ames method is applied to the discrete-tone noise. For fan stages with inlet guide vanes or a preceding fan stage, the basic spectrum level L_c for the discharge duct as given by figure 10(b) is increased by 6 decibels.

Rotor-stator spacing correction. - The correction for rotor-stator spacing specified by the Boeing-Ames method is also applied to the basic spectrum levels (L_c) given by figure 10. The correction is based on the spacing factor RSS defined in figure 6(a). The correction is shown by the solid curve in figure 12 and given by $L = -10 \log_{10} RSS/300$. The correction is applied to both inlet and discharge noise levels.

Inlet flow distortion adjustment. - As previously discussed for broadband noise levels, the effect of rotor-stator spacing on tone generation was not strongly evident in the NASA Lewis fan tests. The suppression of this effect is attributed to the dominance of tones generated by inlet flow distortions. The interim procedure used to account for inlet flow distortion effects on tone levels is identical to that used for broadband noise. The rotor-stator spacing factor RSS is arbitrarily assigned a value of 100 unless, in reality, it is less than 100. This adjustment is shown by the dashed curve in figure 12. This procedure is recommended for all static and ground roll operating conditions.

Directivity correction. - The directivities of the discrete tones propagating from the inlet and discharge duct as established from the NASA Lewis data are shown in figure 13. The directivities specified in the Boeing-Ames method are also shown. The harmonic content of the tones is assumed to remain fixed with polar angle. This representation is not confirmed by the fan noise data that usually show a varying harmonic content with polar angle. This varying behavior has been difficult to correlate and is not yet included in the directivity correction.

Combination-Tone Noise

An additional source of fan noise becomes significant when the tip relative inlet Mach number of a rotor becomes supersonic. At supersonic tip speeds, shock waves are formed at the leading edge of each rotor blade. These shocks move upstream and decay into a system of Mach waves which propagate out of the inlet duct. Ideally, they would be heard in the far field as a blade passage frequency tone. Experience indicates that there is a redistribution of energy. Small differences within the manufacturing and assembly tolerances of rotor blades appear to affect the strength and propagation of the

shocks attached to each blade. Some adjacent shocks coalesce within the duct, and the resulting Mach wave system repeats itself with each revolution of the rotor. The resulting noise spectrum contains harmonics of the shaft rotational speed rather than the blade passage tone alone. These shaft order tones (combination tones) have been termed buzz-saw noise for the subjective response they produce. This type of noise is found in fans and compressors which operate at supersonic tip speeds, but it may be masked by a louder tone at the blade-passage frequency or by jet noise. The exact characterization of combination-tone noise is difficult because duplicate fans can exhibit different noise signatures due to manufacturing tolerances and changes caused by usage.

The method of predicting combination-tone noise specified in the Boeing-Ames method is adopted with modifications based on the NASA Lewis fan data. The modifications consist of level and directivity adjustments which conform to the NASA Lewis results with fan C. Spectral content specified in the Boeing-Ames method is maintained. Some of these adjustments are considered to be substantial and, in view of the limited data base for combination-tone noise from the NASA Lewis data, must be considered tentative until a larger sample of results is examined.

Spectrum content. - The combination-tone noise is characterized by three separate spectra as specified in the Boeing-Ames method and shown in figure 14. Each spectra peaks at a different frequency. The peak noise levels of the three spectra center at one-half, one-fourth, and one-eighth of the fundamental blade passage frequency of the first fan stage.

Spectrum level. - The levels of the three spectra are characterized as shown in figure 15. Both the modified behavior based on the NASA Lewis data (fig. 15(a)) and that of the Boeing-Ames method (fig. 15(b)) expressed in terms of the normalized levels used in this report are shown.

Inlet-guide-vane correction. - A correction is applied to the combination-tone noise levels for fans with inlet guide vanes. The level is reduced by 5 decibels for such fans. This attenuating effect of inlet guide vanes differs from that specified in the Boeing-Ames method wherein it is taken that the vanes completely eliminate the combination tone noise.

Directivity correction. - The combination-tone noise is assumed to radiate only from the fan inlet duct. The directivity of the radiation is given in figure 16. The directivity specified in the Boeing-Ames method is also shown. The directivity from the NASA Lewis data shows that the combination-tone noise persists at a reduced level throughout the rear quadrant of fan.

PREDICTION PROCEDURE

A calculation procedure is presented in detail for predicting the noise for one stage of a fan or compressor based on previous presentations and figures. The noise from a compressor of a turbojet engine involves only a prediction of the noise radiating from the inlet duct for the first compression stage. A prediction of the noise produced by two-stage fans of turbofan engines requires that an energy sum be made of the noise predicted for each stage. Application of the prediction method for fans with more than two stages is not recommended because blade row attenuation is not considered.

The procedure for predicting the noise radiated from the inlet and discharge ducts of a stage are presented separately. In each case, procedures are described for predicting the noise components (broadband, discrete tone, and combination tone, when applicable). An energy sum of these noise components is required to obtain the total noise. The calculations provide the one-third octave sound pressure levels of the free-field noise pattern at a 1-meter radius.

Fan and Compressor Inlet Noise

Broadband noise. - The characteristic one-third octave band sound pressure level of a single fan stage is given by

$$L_c = 20 \log_{10} \left(\frac{\Delta T}{\Delta T_o} \right) + 10 \log_{10} \left(\frac{\dot{m}}{\dot{m}_o} \right) + F_1 \left[(M_{TR}), (M_{TR})_D \right] + F_2(RSS) + F_3(\theta) \quad (4)$$

where F_1 and F_3 are the functions represented by the appropriate curves in figures 4(a) and 7(a), respectively, and F_2 is the function represented in figure 6(b) appropriate for fan operation with or without inlet flow distortion (flight or static and ground roll operation).

The sound pressure level spectrum is obtained from

$$SPL(f) = L_c + F_4 \left(\frac{f}{f_b} \right) \quad (5)$$

where F_4 is represented by the curve in figure 3(a) or equation (2).

Discrete-tone noise. - The characteristic peak level for the fundamental tone is given by

$$L_c = 20 \log_{10} \left(\frac{\Delta T}{\Delta T_o} \right) + 10 \log_{10} \left(\frac{\dot{m}}{\dot{m}_o} \right) + F_1 \left[(M_{TR}), (M_{TR})_D \right] + F_2(RSS) + F_3(\theta) \quad (6)$$

where F_1 and F_3 are represented by the appropriate curves in figures 10(a) and 13(a), respectively, and F_2 is represented by the curve in figure 12 appropriate for fan operation with or without inlet flow distortions (flight or static and ground roll operation).

The sound pressure level of the discrete-tone harmonics is obtained as an energy sum of the tone levels from rotor-stator interaction tones and inlet flow distortion tones when applicable:

$$\text{SPL}(f) = L_c + 10 \log_{10} \left[10^{0.1F_4(f/f_b)} + 10^{0.1F_5(f/f_b)} \right] \quad (7)$$

where F_4 is represented by the function in figure 8 appropriate for fan stages with or without inlet guide vanes and with or without fundamental tone cutoff. Cutoff occurs when δ , as calculated from equation (3), is less than 1.05. And F_5 represents the function in figure 9 for first-stage fans with inlet flow distortions (static and ground roll operation). Without inlet flow distortions and for any second fan stage, $F_5(f/f_b)$ should be neglected.

Combination-tone noise. - Combination-tone noise is calculated only for first-stage fans. The characteristic peak level at center frequencies one-half, one-fourth, and one-eighth of the fundamental blade passage frequency f_b is given by

$$L_c = 20 \log_{10} \left(\frac{\Delta T}{\Delta T_o} \right) + 10 \log_{10} \left(\frac{\dot{m}}{\dot{m}_o} \right) + F_1 \left[(M_{TR}) \right] + F_2(\theta) + C \quad (8)$$

where F_1 is represented by the appropriate curve for f/f_b equal to 1/2, 1/4, and 1/8 in figure 15(a); F_2 is represented by the curve in figure 16; C equals -5 decibels for first-stage fans with inlet guide vanes and 0 decibels for first-stage fans without inlet guide vanes.

The sound pressure level spectrum for each of the three combination tone sub-components is given by

$$\text{SPL}(f) = L_c + F_3 \left(\frac{f}{f_b} \right) \quad (9)$$

where F_3 is represented by the appropriate curve for one-half, one-fourth, and one-eighth of the blade passage frequency in figure 14.

The sound pressure levels of the three combination tone noise spectra obtained by the preceding procedure are added on an energy basis to give the total combination tone noise sound pressure level spectrum.

Fan Discharge Noise

Broadband noise. - The characteristic one-third octave band sound pressure level of a single fan stage is given by

$$L_c = 20 \log_{10} \left(\frac{\Delta T}{\Delta T_o} \right) + 10 \log_{10} \left(\frac{\dot{m}}{\dot{m}_o} \right) + F_1 \left[(M_{TR}), (M_{TR})_D \right] + F_2(RSS) + F_3(\theta) + C \quad (10)$$

where F_1 and F_3 are represented by the appropriate curves in figures 4(b) and 7(b), respectively; F_2 is represented by the curve in figure 6(b) appropriate for fan operation with or without inlet flow distortions (flight or static and ground roll operation); and C equals 3 decibels for fan stages with inlet guide vanes or for second-stage fans and is neglected otherwise.

The sound pressure level spectrum is obtained by

$$SPL(f) = L_c + F_4 \left(\frac{f}{f_b} \right) \quad (11)$$

where F_4 is represented by the curve in figure 3(a) or equation (2).

Discrete-tone noise. - The characteristic peak level for the fundamental tone is given by

$$L_c = 20 \log_{10} \left(\frac{\Delta T}{\Delta T_o} \right) + 10 \log_{10} \left(\frac{\dot{m}}{\dot{m}_o} \right) + F_1 \left[(M_{TR}), (M_{TR})_D \right] + F_2(RSS) + F_3(\theta) + C \quad (12)$$

where F_1 and F_3 are represented by the appropriate curves in figures 10(b) and 13(b), respectively; F_2 is represented by the curve in figure 12 appropriate for fan operation with or without inlet flow distortions (flight or static and ground roll operation); and C equals 6 decibels for fan stages with inlet guide vanes or for second-stage fans and is neglected otherwise.

The sound pressure level of the discrete tone harmonics is given by

$$SPL(f) = L_c + F_4 \left(\frac{f}{f_b} \right) \quad (13)$$

where F_4 represents the function in figure 8 appropriate for the fan stages with or without inlet vanes or with or without fundamental tone cutoff. Cutoff occurs when δ , as calculated from equation (3), is less than 1.05.

PREDICTED AND EXPERIMENTAL COMPARISONS

Comparisons of the predicted and experimental far-field noise properties are presented for the eight full-scale single-stage NASA Lewis fans which were used as the data base for modifications to the Boeing-Ames prediction method. Table I shows some of the design properties of these fans. A general discussion of the acoustic and design properties of the fans is presented in reference 3. Predicted and experimental comparisons will be presented for four-speed conditions for each fan. The speeds cover the 60 to about 90 percent of design speed operating conditions used during the acoustic testing of the fan.

The comparisons consist of both detailed far-field and overall acoustic properties. Figure 17 compares predicted and experimental sound power levels, and figure 18 compares the perceived noise levels at a sideline distance of 304.8 meters (1000 ft). The calculations of sound power and perceived noise levels are made using the data handling procedures described in reference 13. The perceived noise levels include the effects of atmosphere attenuation. Figure 19 shows the predicted and measured sound pressure spectra at 16 angular positions referenced to a 1-meter radius for each of the fans.

The accuracy of the overall level of the noise predictions will be considered first. Figure 17(a) shows the total sound power level to be predicted to within an accuracy of better than ± 1 decibel. Figures 17(b) and (c), which compare the sound power level in the inlet and discharge quadrant of the far-field noise pattern, show that the accuracy for the discharge noise appears somewhat better than that for the inlet, but an accuracy of about ± 1 decibel is maintained for both quadrants.

The perceived noise levels are more sensitive to spectral detail than the sound power levels and provide a more critical test of the prediction method. Comparisons of the predicted and experimental perceived noise levels for the 40° polar angle in the inlet quadrant and 120° in the discharge quadrant are shown in figures 18(a) and (b), respectively. Experimentally, the maximum perceived noise levels occurs at or near these polar angles. The accuracy of predicting perceived noise levels is about ± 2 decibels, although there are exceptions where it exceeds these limits. Both the prediction method and any nontypical operation of the fans will require additional attention in examining these exceptions.

The most critical test of the prediction method involves the far-field spectral patterns shown in figure 19. It should initially be noted that the low-frequency region of the spectra (the region up to the fundamental blade passage tone) should be ignored in any comparison. The experimental data exhibit jet noise properties in the low-frequency region, and jet noise was not considered in the prediction method. In the frequency region dominated by fan noise, the spectral comparisons range from

extremely good to very poor depending on the specific fan and polar angle being examined. One of the reasons for presenting the entire array of comparison in figure 19 is the difficulty in selecting representative comparisons which demonstrate the precision of the prediction method. A comparison could be selected which would weight an evaluation in any direction and to whatever degree desired. Figure 19 is provided to allow the reader to evaluate the prediction method from a variety of viewpoints.

In general, it is obvious that the prediction method will not provide the detailed variations in the spectra from angle to angle and from fan to fan exhibited by the experimental data. In most instances, however, the trends exhibited by the data are adequately predicted. The exceptions will probably require the identification of more noise control parameters than were used in the interim prediction method. For example, the absence of discrete tones for the 60-percent speed condition of fan A (fig. 19(a)) is not predicted. Neglecting inlet flow distortions for this cutoff condition could better simulate the data. However, either the lack of distortions or the effect of some other variable remains to be identified. There are other instances in the comparisons where unique experimental behavior must be investigated.

One encouraging result of the prediction method include the modifications of the Boeing-Ames method with regard to blade passage frequency cutoff and inlet flow distortion effects. All the fans except QF-6, QF-9, and C at high speeds are calculated to exhibit cutoff behavior. In general, the cutoff fans experimentally exhibit a prominent tone in the inlet quadrant and a suppressed tone in the discharge quadrant. The predicted spectra simulate this behavior as a result of the cutoff and inlet flow distortion modifications incorporated into the prediction procedure. Although the results are encouraging, a more definitive description of distortion-related noise is needed so that distortion can be treated as a continuous, rather than an on-off, parameter.

An inspection of the fan C spectra in figure 19 illustrates the changing behavior of combination noise with a change in fan speed. The interim method predicts the approximate levels of combination tone noise, but the predicted noise lacks some of the spectral detail of the experimental data. In effect, the 90-percent speed conditions for fans A and B also provide an evaluation of combination-tone noise predictions. A low level is predicted which is comparable to that inferred by the experimental data. In contrast, a much higher level was predicted by the Boeing-Ames method for their fans. These limited results, however, mostly emphasize the need of a broader data base to formulate combination-tone prediction procedures.

These comparisons of predicted and experimental noise properties illustrate the accuracy and limitations of the interim prediction method. Sound power and perceived noise levels are predicted to within about ± 2 decibels, an accuracy adequate for many NASA applications. The method provides the general properties of the far-field noise spectra which are useful for many purposes. However, much of the spectral detail is

not predicted. In general, the intended purposes of the interim prediction method are satisfied.

CONCLUDING REMARKS

One of the limitations of the interim prediction method concerns the data base used to formulate the method. The data base consists of a partial noise data analysis restricted to full-scale fans tested on an outdoor facility at NASA Lewis. Although this data base is more extensive than that from any other source, a more detailed noise component analysis of data from a broader spectrum of fans and test facilities is needed. In particular, multistage fan and compressor noise data must be examined. One of the first steps in upgrading the prediction method should be an evaluation of the method for a broader spectrum of fan noise data. The deficiencies of the method revealed by such evaluations would provide the best guidance for the direction and emphasis of additional modifications.

Although the quantity of the data base is important, the quality of this data base is of much greater concern at this time. The data base currently available for prediction methods is almost exclusively acquired from ground static tests of fans. It has been established with some certainty (e.g., refs. 14 and 15) that inlet flow distortions which exist during static testing can cause substantial differences in the noise properties between static and flight tests. The distortion-related noise may dominate the noise spectra and override much of the noise which occurs only in flight. An attempt to partially account for the distortion-related noise during static tests was incorporated in a qualified manner in the interim prediction method. Much additional effort toward evaluating flow distortion effects must be exerted and given immediate attention. The distortion-related noise is expected to have different parameter dependencies than rotor-stator interactions or other noise sources. If, in fact, distortion noise dominates the noise signature during static tests, the data may be useless for flight noise predictions. Hopefully, the dominance in most cases is not severe. A quantitative evaluation of distortion-related noise is needed to assure success in upgrading the interim prediction method by a more extensive examination of static test noise data. No significant improvement in the accuracy of noise prediction methods can be expected without the quantitative identification or elimination of distortion-related noise from the data base used to formulate the prediction method.

Presuming that progress will be made in identifying distortion-related noise, a revision of the prediction method is recommended as an immediate upgrading effort. The revision consists of incorporating distortion-related noise as separate noise sources in the method. The sources should consist of broadband and discrete-tone

noise for both the inlet and discharge ducts. The addition of these four sources doubles the sources currently described, because distortion effects are currently treated as a correction to interaction noise. The advantage of multiple sources, even though the distortion sources are marginally described, is that a prediction procedure with multiple sources is more realistic and flexible. The procedure could allow for a degree of distortion noise to be specified rather than the on-off criteria currently used. Rotor-stator spacing effects could also be predicted more realistically for static and ground roll operation. Although these revisions of the prediction method would give only marginal changes in accuracy at this time, the method would be a more versatile and realistic vehicle for incorporating and testing the eventual descriptions of noise related to inlet flow distortion.

REFERENCES

1. Dunn, D. G.; and Peart, N. A.: Aircraft Noise Source and Contour Estimation. (D6-60233, Boeing Commercial Airplane Co.; NAS2-6969.) NASA CR-114649, 1973.
2. Feiler, C. E.; and Conrad, E. W.: Noise from Turbomachinery. AIAA Paper 73-815, Aug. 1973.
3. Heidmann, M. F.; and Feiler, C. E.: Noise Comparisons From Full-Scale Fan Tests at NASA Lewis Research Center. AIAA Paper 73-1017, Oct. 1973.
4. Aircraft Engine Noise Reduction. NASA SP-311, 1972.
5. Smith, M. J. T.; and House, M. E.: Internally Generated Noise from Gas Turbine Engines. Measurement and Prediction. ASME Trans., vol. 89, no. 1, Jan. 1967, pp. 117-190.
6. Burdsall, E. A.; and Urban, R. H.: Fan-Compressor Noise: Prediction, Research and Reduction Studies. Pratt and Whitney Aircraft (FAA-RD-71-73), 1971.
7. Benzakein, M. J., et al.: Fan/Compressor Noise Research. General Electric Co. (FAA-RD-71-85), 1971.
Vol. I - Detailed Discussion, AD-740513.
Vol. II - Detailed Discussion, AD-740514.
Vol. III - Compilation of Test Data, AD-740515.
Vol. IV - Compilation of Test Data, AD-740516.
8. Metzger, F. B.; and Hanson, D. B.: Low Pressure Ratio Fan Noise Experiment and Theory. ASME Paper 72-GT-40, Mar. 1972.

9. Brines, Gerald L.: Studies for Determining the Optimum Propulsion System Characteristics for Use in a Long Range Transport Aircraft. (PWA-4449, Pratt and Whitney Aircraft; NAS3-15550.) NASA CR-120950, 1972.
10. Propulsion System Studies for the Advanced High Subsonic, Long Range Jet Commercial Transport Aircraft. (R72-AEG-296, General Electric Co.; NAS3-15544. NAS3-15544.) NASA CR-121016, 1972.
11. Helms, H. E.: Quiet Clean STOL Experimental Engine Study Program (Task II - Preliminary Design Studies). EDR-7610, Detroit Diesel Allison, 1972.
12. Tyler, J. M.; and Sofrin, J. E.: Axial Flow Compressor Noise Studies. SAE Trans., vol. 70, 1962, pp. 309-332.
13. Montegani, Francis J.: Some Propulsion System Noise Data Handling Conventions and Computer Programs Used at the Lewis Research Center. NASA TM X-3013, 1974.
14. Cumsty, N. A.; and Lowrie, B. W.: The Cause of Tone Generation by Aeroengine Fans at High Subsonic Tip Speeds and the Effect of Forward Speed. ASME Paper 73-WA-GT-4, Nov. 1973.
15. Feiler, C. E.; and Merriman, J. E.: Effects of Forward Velocity and Acoustic Treatment on Inlet Fan Noise. AIAA Paper 74-946, Aug. 1974.

TABLE I. - NASA LEWIS RESEARCH CENTER FULL-SCALE FAN DESIGN PROPERTIES

Fan	Total pressure	Mass flow rate, m		Rotor tip Mach number, M_T	Rotor tip relative inlet Mach number, $(M_{TR})_D$	Number of vanes	Number of blades	Blade passage frequency, f_b , Hz	Cutoff factor (eq. (3)), δ	Rotor-stator spacing factor, RSS, percent
		kg/sec	lb/sec							
A	1.5	430	950	1.04	1.20	90	40	2420	0.83	200
B	1.5	430	950	1.04	1.20	60	26	1570	.80	200
C	1.6	415	915	1.39	1.52	60	26	2250	----	200
QF-1	1.5	396	873	.99	1.12	112	53	3120	.89	367
QF-3	1.4	396	873	.99	1.12	112	53	3120	.89	367
QF-5	1.6	385	850	.98	1.14	88	36	2180	.68	227
QF-6	1.2	396	873	.67	.88	50	42	1670	3.53	400
QF-9	1.2	403	889	.63	.87	11	15	556	2.38	200

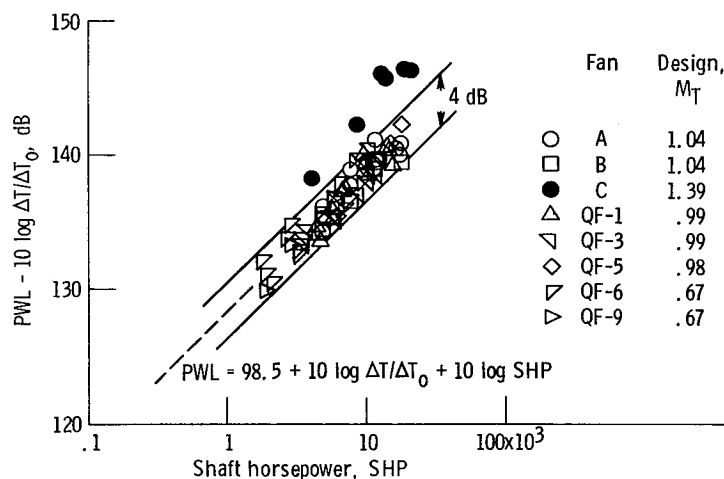


Figure 1. - Correlation of total sound power levels for NASA Lewis full-scale fan data (ref. 3).

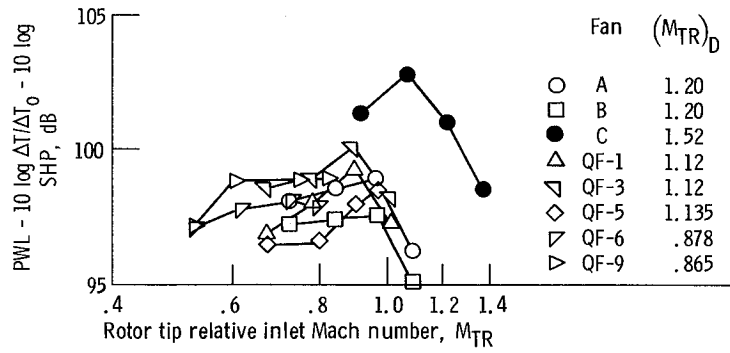
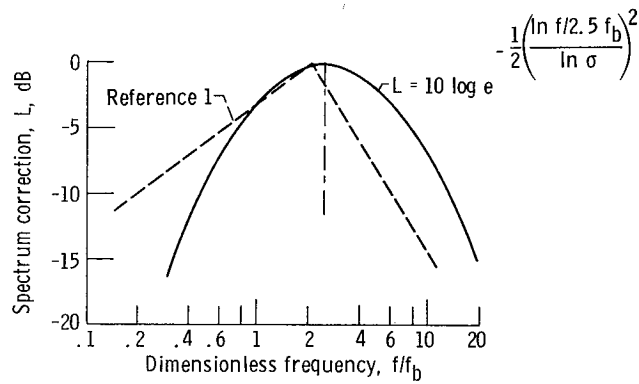
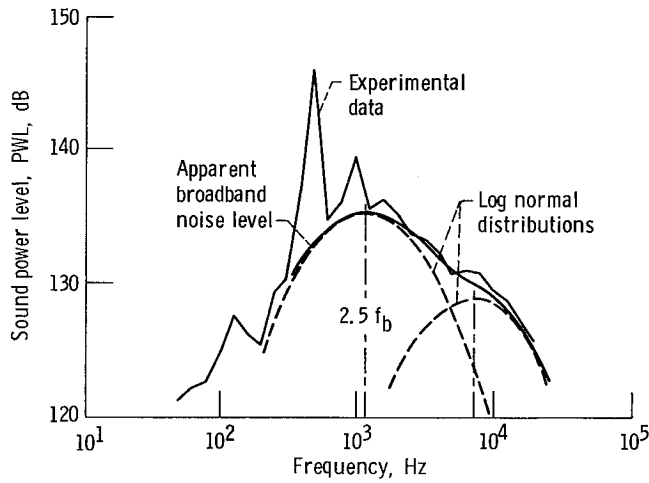


Figure 2. - Total sound power level variations for NASA Lewis full-scale fan data.



(a) Broadband noise spectrum content.



(b) Example of bimodal broadband properties from NASA Lewis full-scale fan tests (ref. 3).

Figure 3. - Broadband noise spectrum properties.

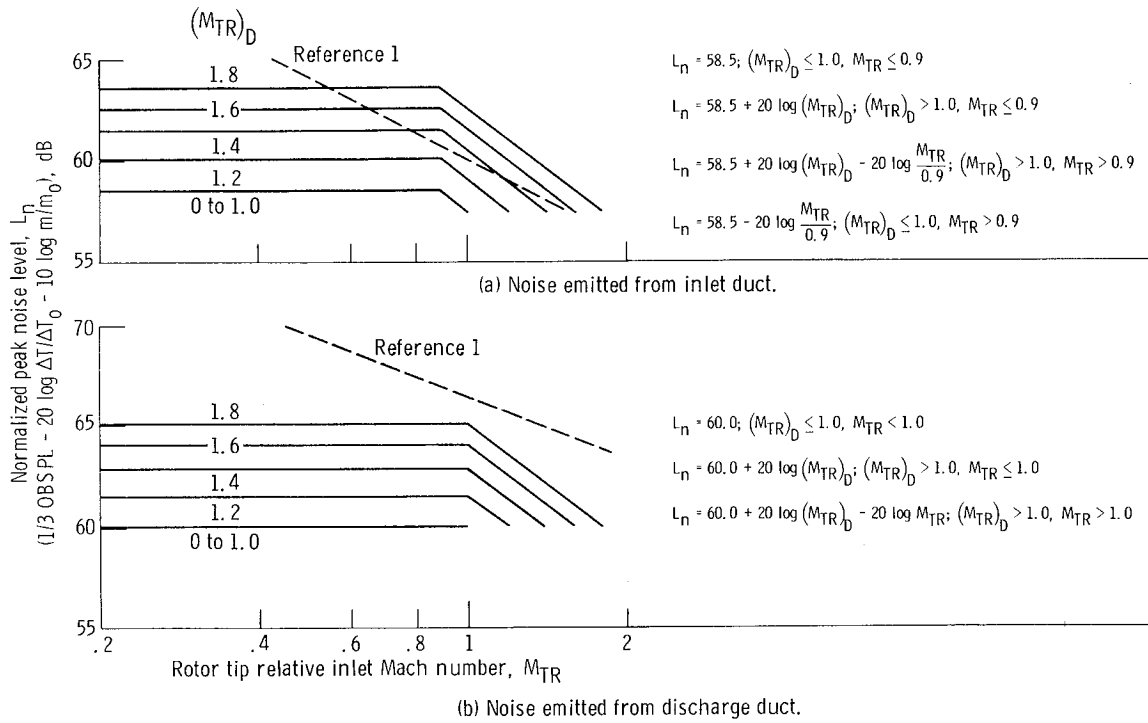


Figure 4. - Peak broadband sound pressure levels from NASA Lewis data analysis.

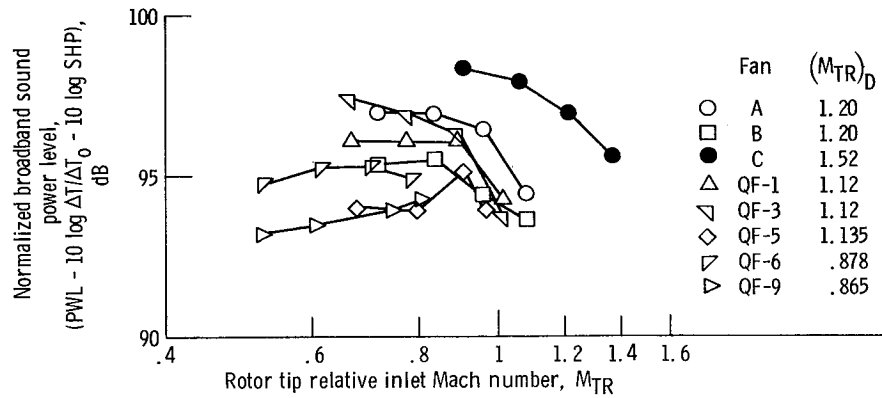
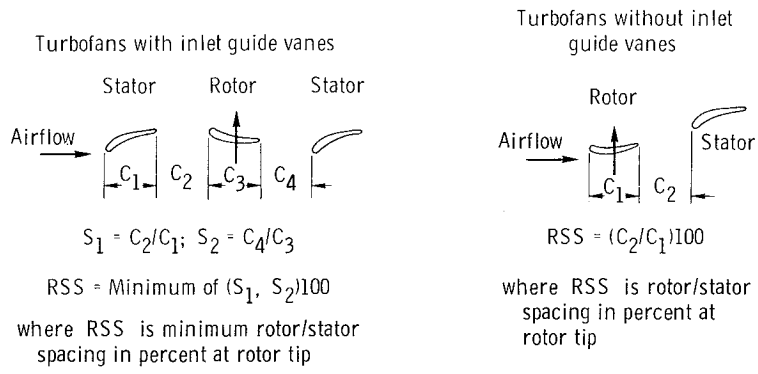
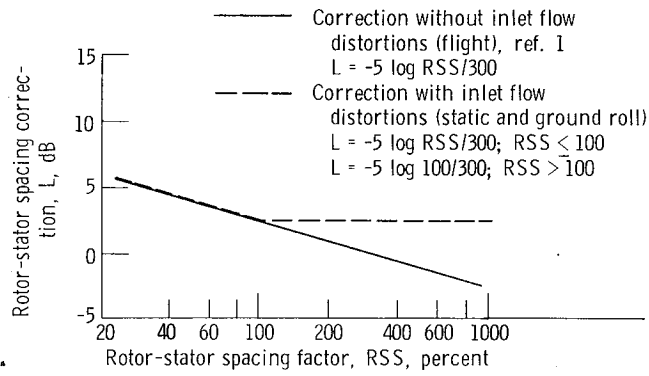


Figure 5. - Broadband power level variations for NASA Lewis full-scale fan data. Maximum operation at 90 percent of design speed.

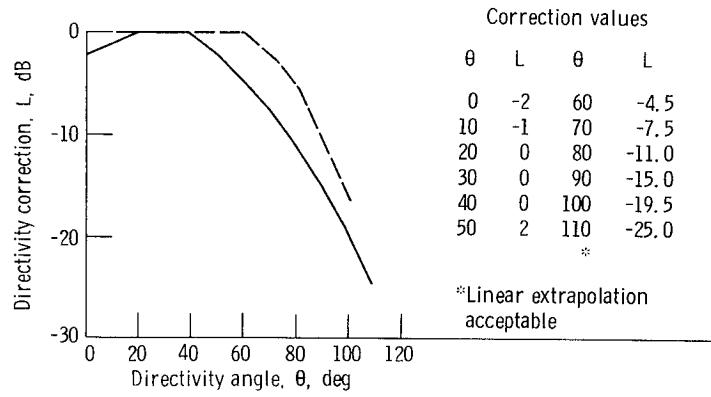


(a) Rotor-stator spacing definition (ref. 1).

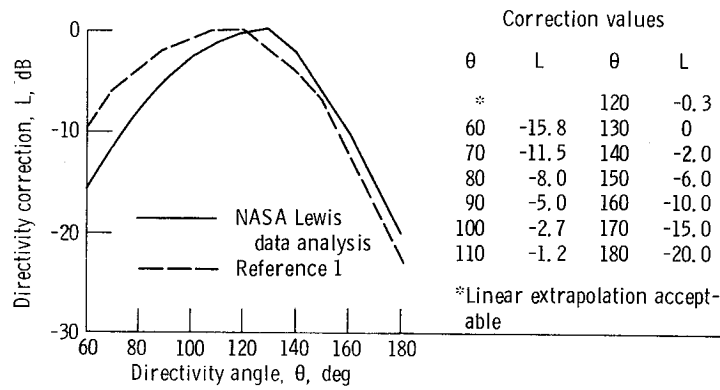


(b) Correction for broadband noise.

Figure 6. - Rotor-stator spacing correction.



(a) Inlet duct.



(b) Discharge duct.

Figure 7. - Directivity corrections for broadband noise.

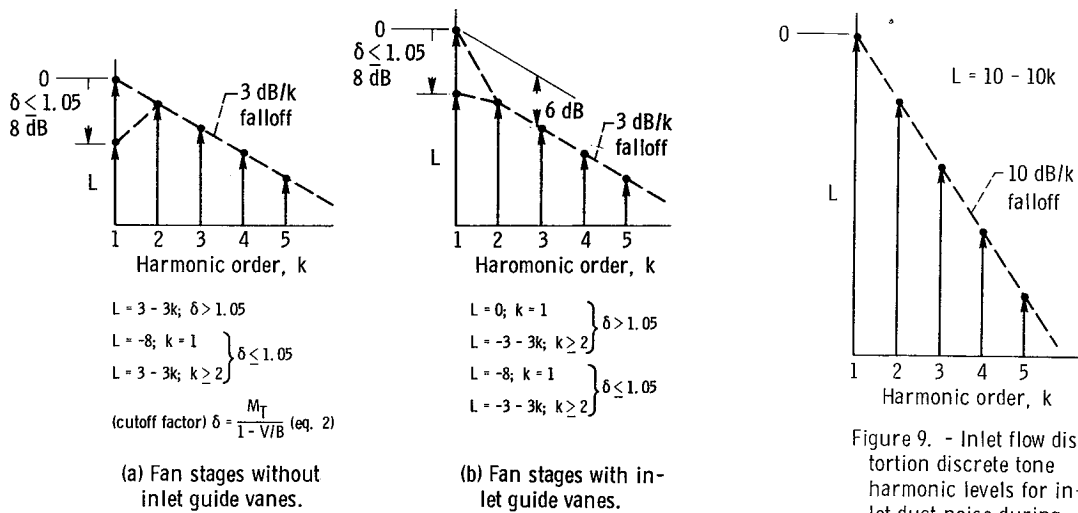


Figure 8. - Rotor-stator interaction discrete tone harmonic levels. (Ref. 1 modified by fundamental tone cutoff correction from NASA Lewis data analysis.)

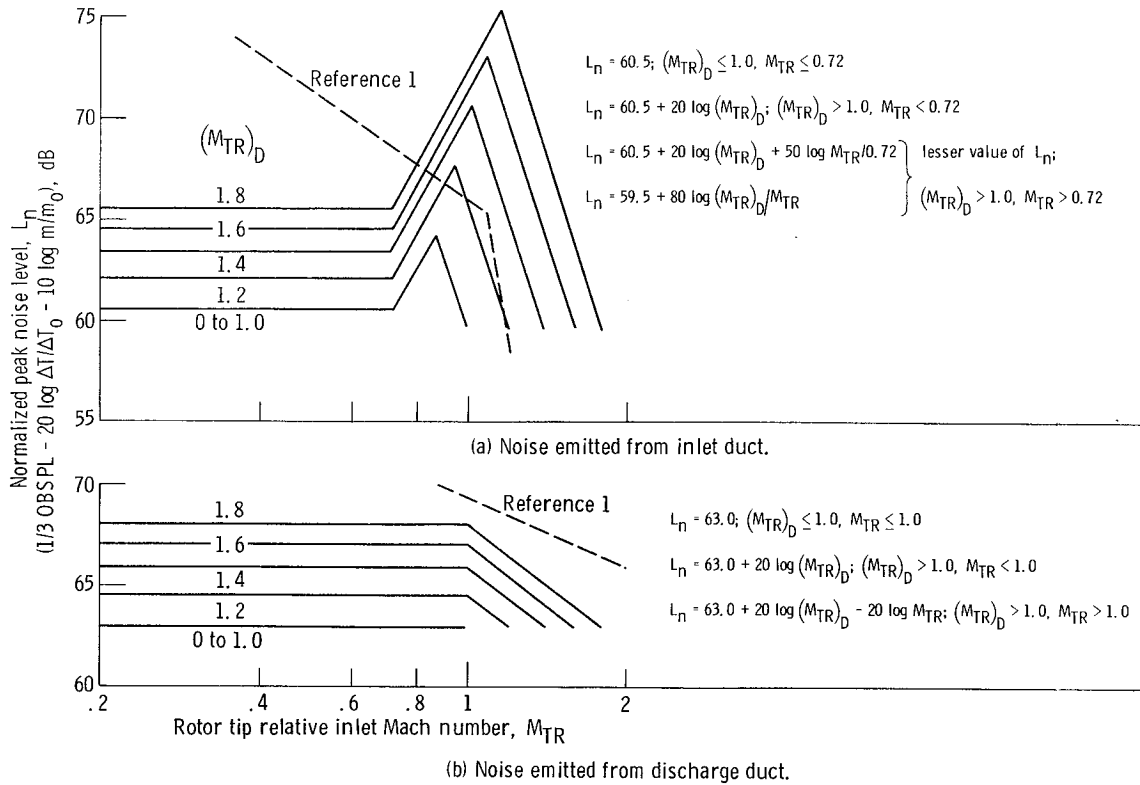


Figure 10. - Characteristic peak sound pressure levels of fundamental discrete tone from NASA Lewis data analysis.

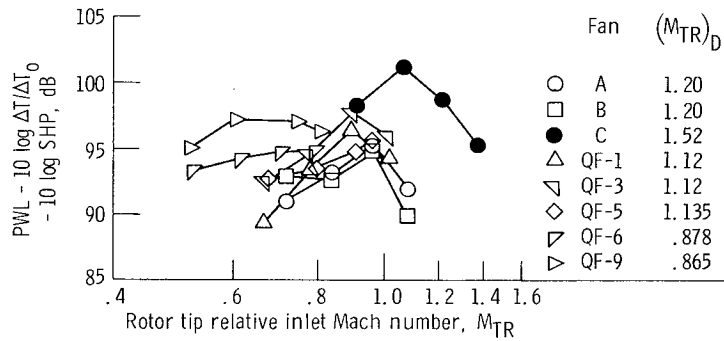


Figure 11. - Discrete tone power level variations for NASA Lewis full-scale fan data.

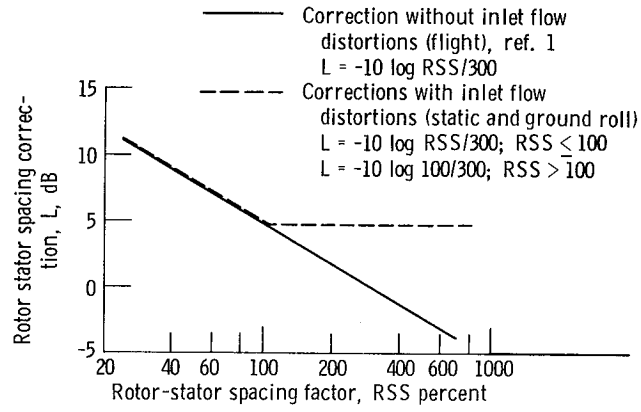
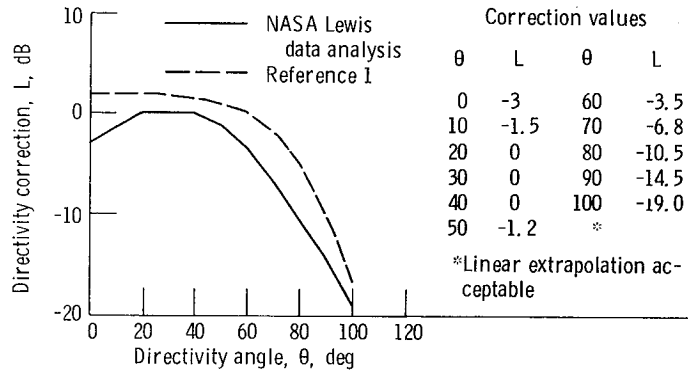
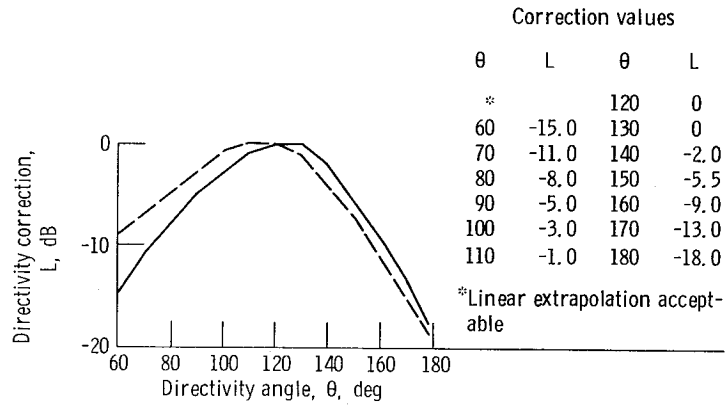


Figure 12. - Rotor-stator spacing correction for discrete tones.



(a) Inlet duct.



(b) Discharge duct.

Figure 13. - Directivity corrections for discrete tones.

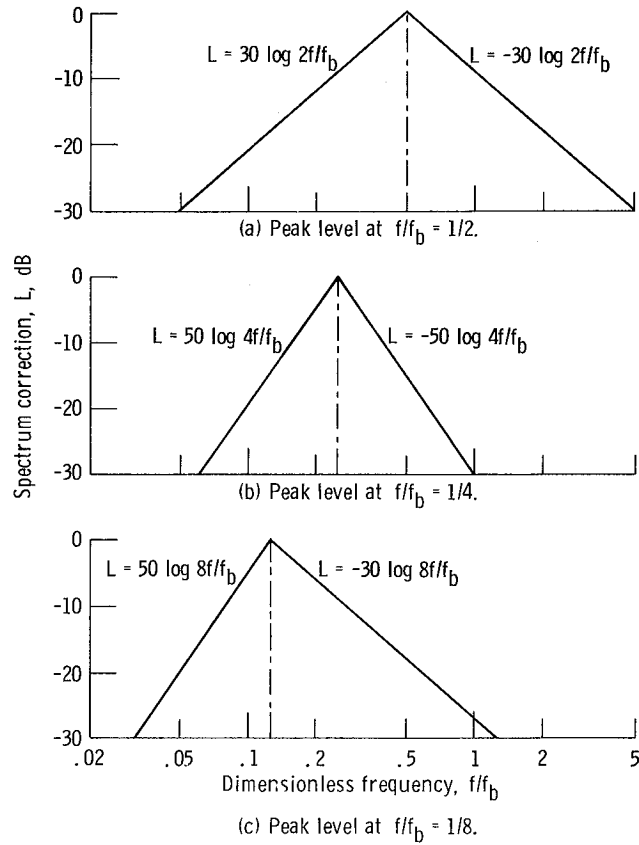
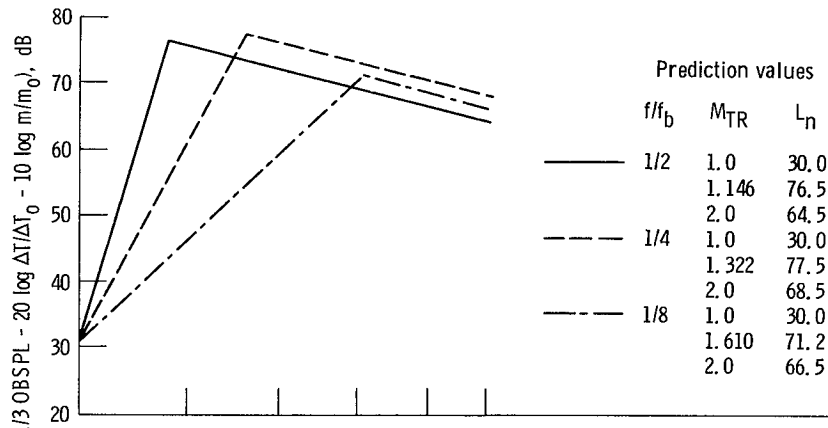
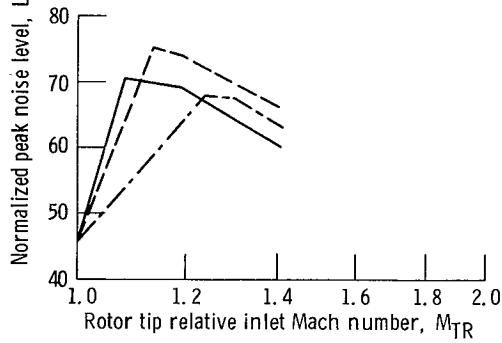


Figure 14. - Combination tone noise spectrum content (ref. 1).



(a) NASA Lewis data analysis.



(b) Reference 1 prediction method.

Figure 15. - Combination tone noise levels at 1/2, 1/4, and 1/8 of blade passage frequency.

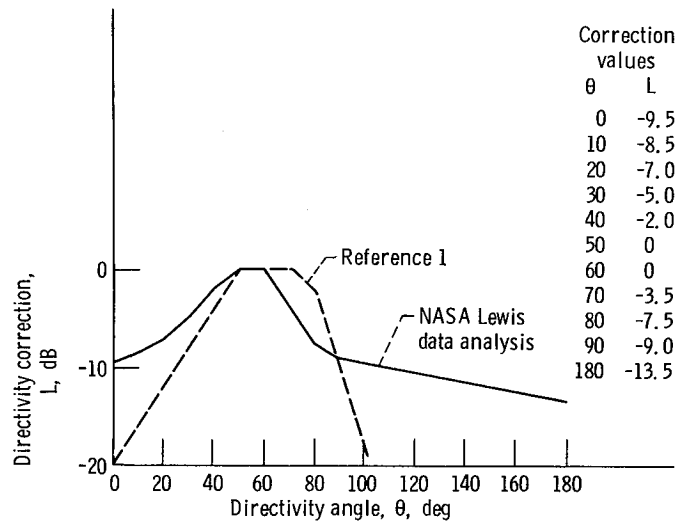
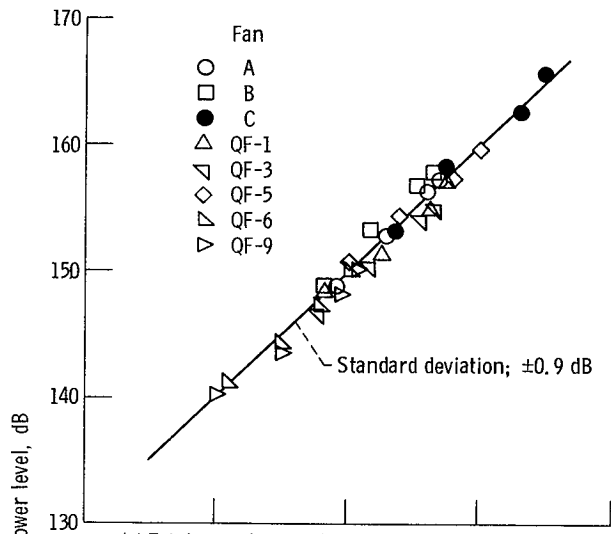
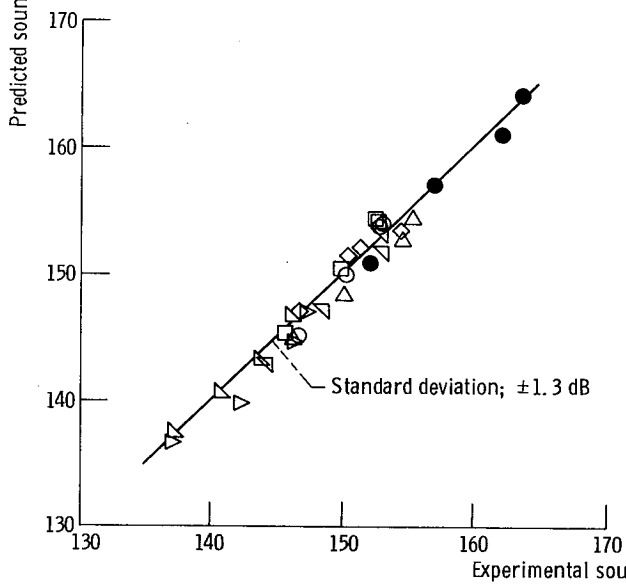


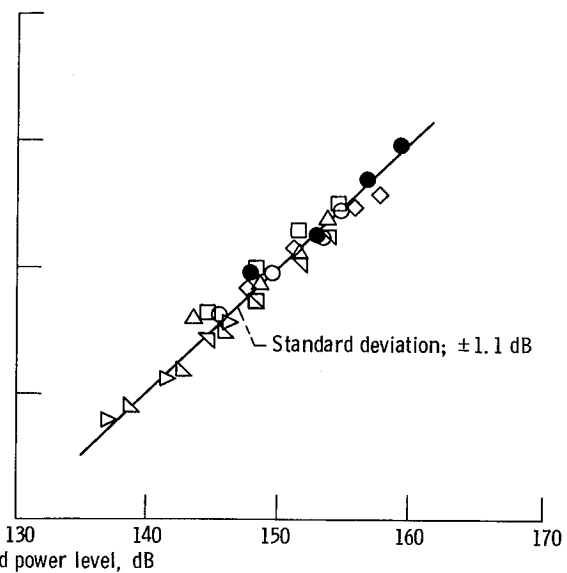
Figure 16. - Directivity correction for combination tone noise.



(a) Total sound power level (inlet plus discharge).



(b) Inlet quadrant sound power level.



(c) Discharge quadrant sound power level.

Figure 17. - Comparison of predicted and experimental sound power levels for NASA Lewis full-scale fans.

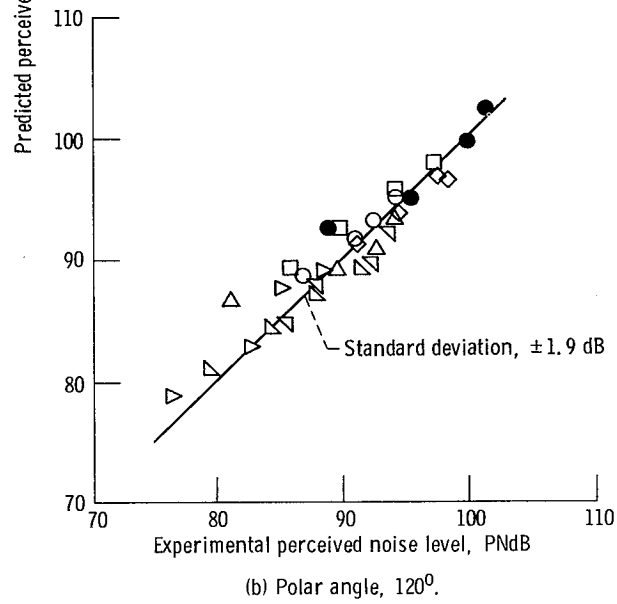
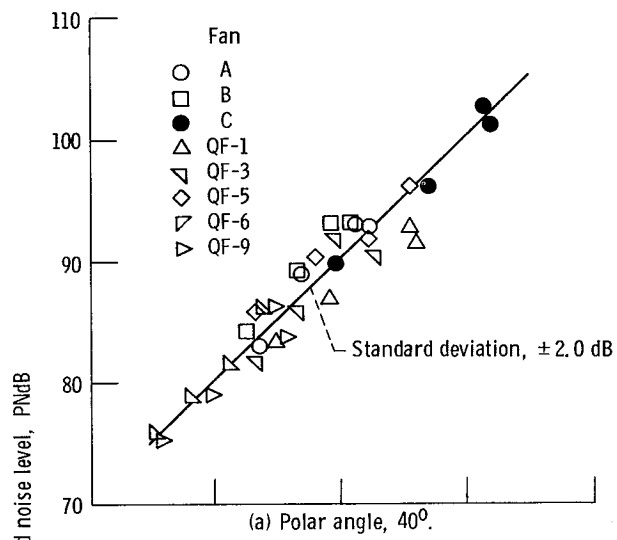
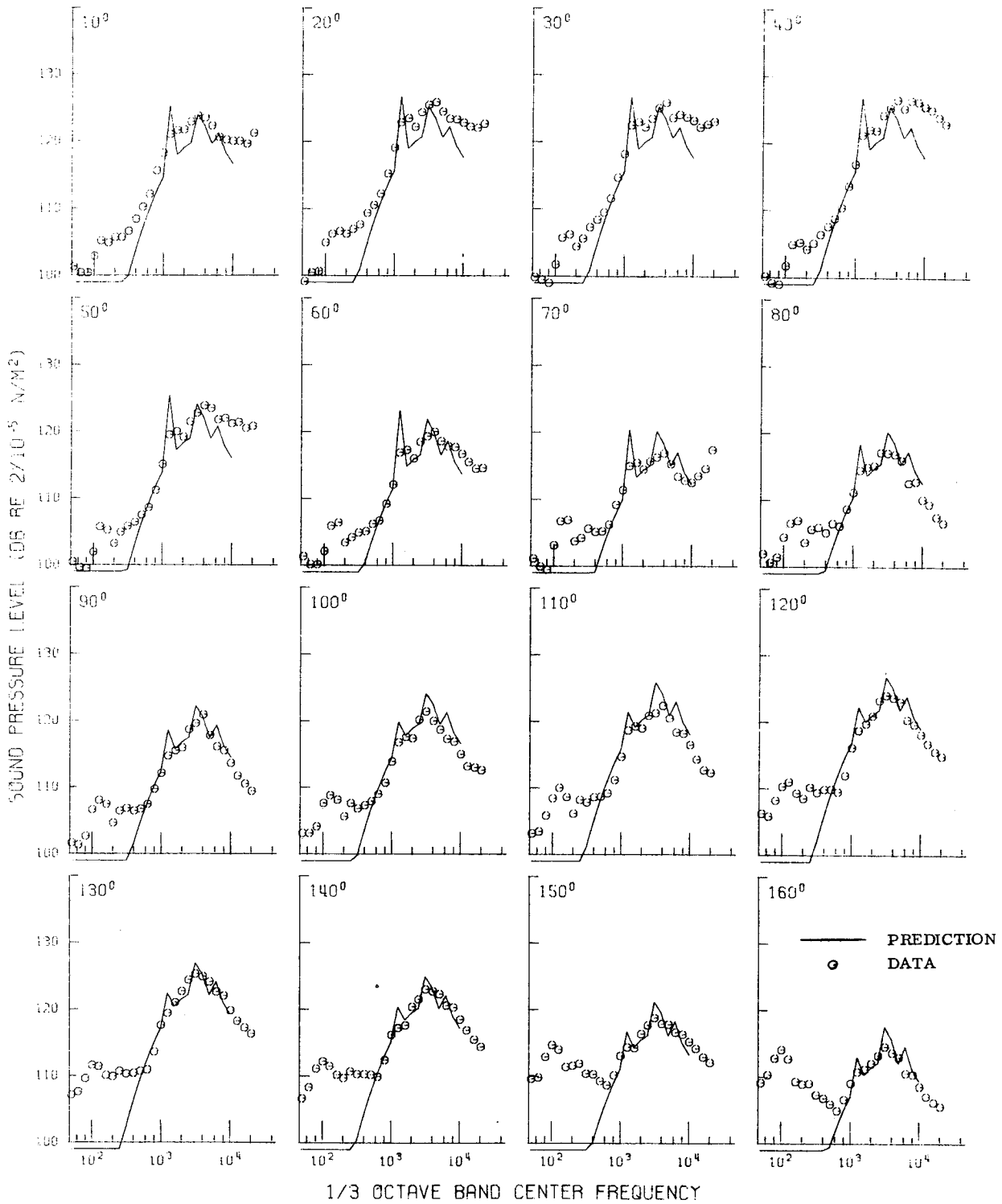
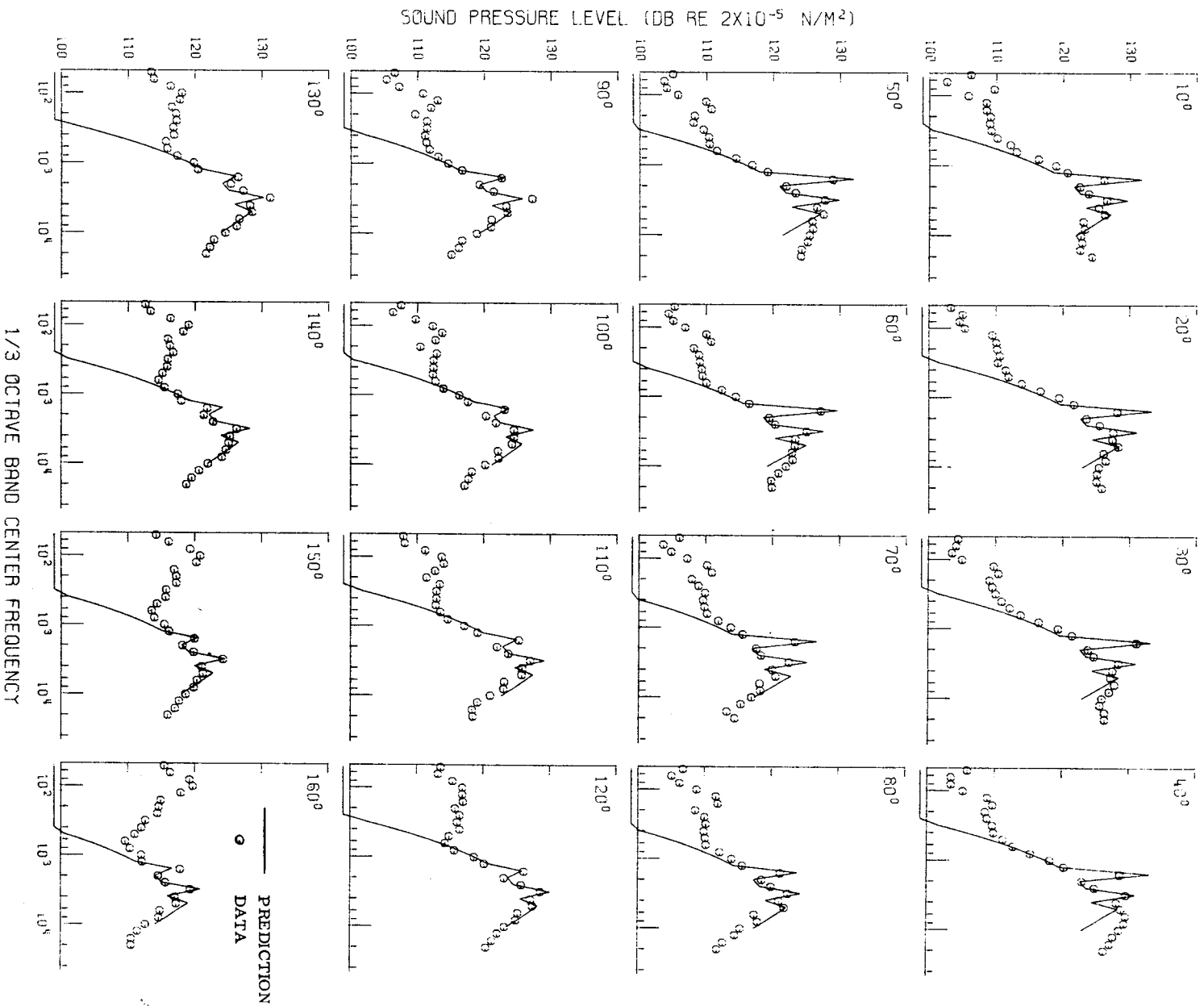


Figure 18. - Comparison of predicted and measured 304.8-meter (1000-ft) sideline perceived noise levels of NASA Lewis fans.



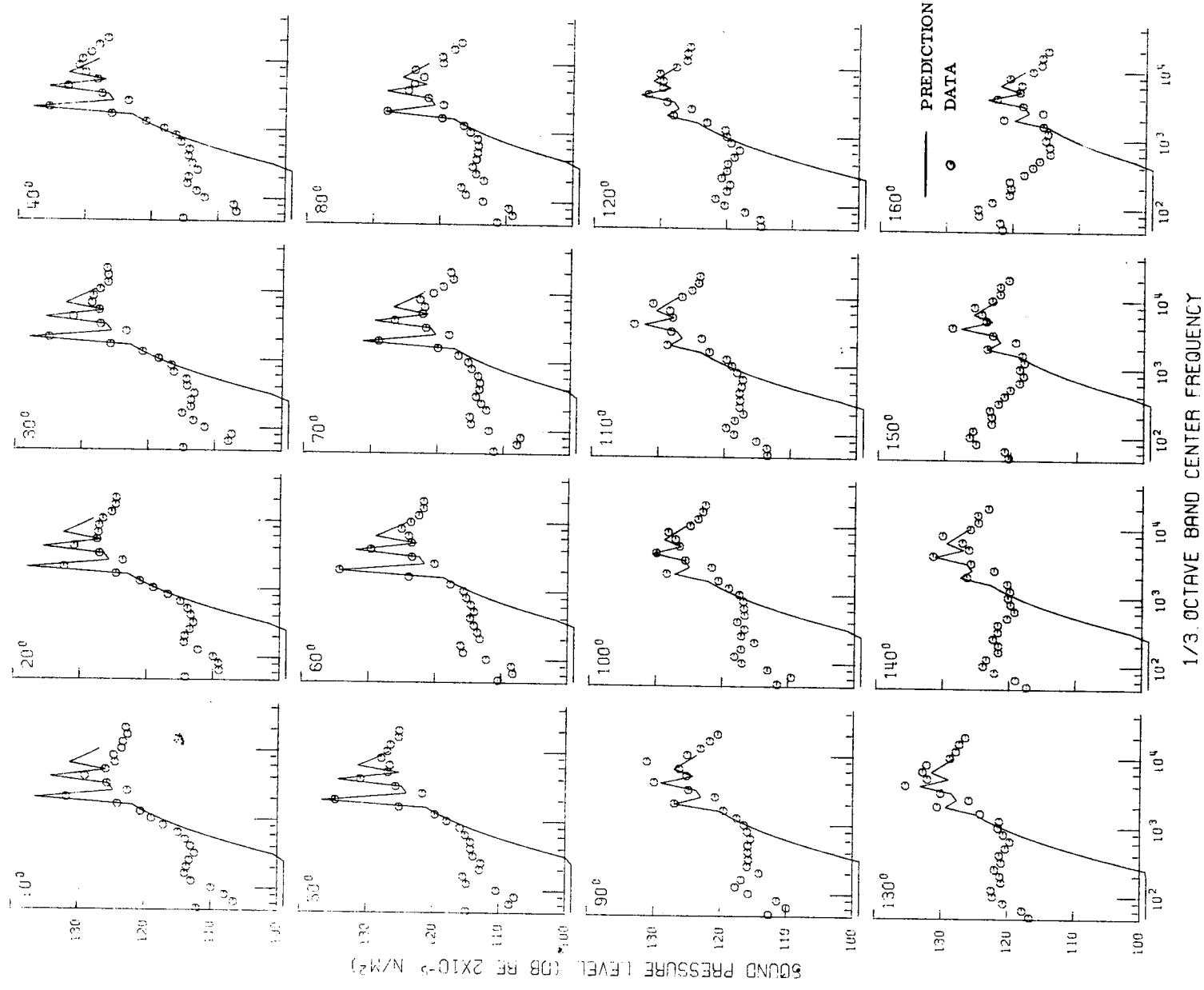
(a) Fan A, configuration 203, 60-percent speed.

Figure 19. - Comparisons of predicted and experimental 1-meter radius sound pressure level spectra at 16 polar angles for NASA Lewis full-scale fans. Comparisons for eight fans each at four operating speeds are presented.



(b) Fan A, configuration 203, 70-percent speed.

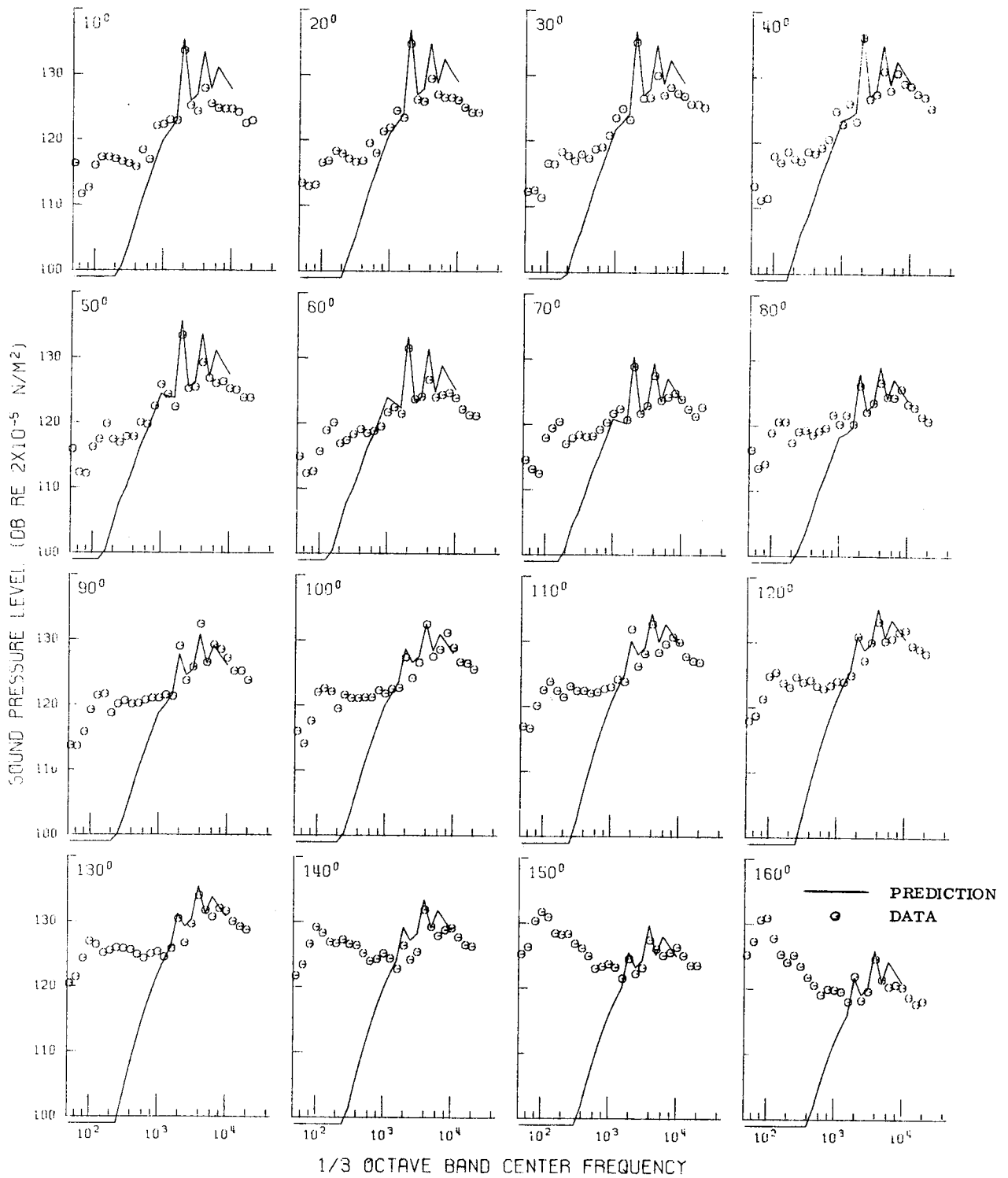
Figure 19. - Continued.



1/3 OCTAVE BAND CENTER FREQUENCY

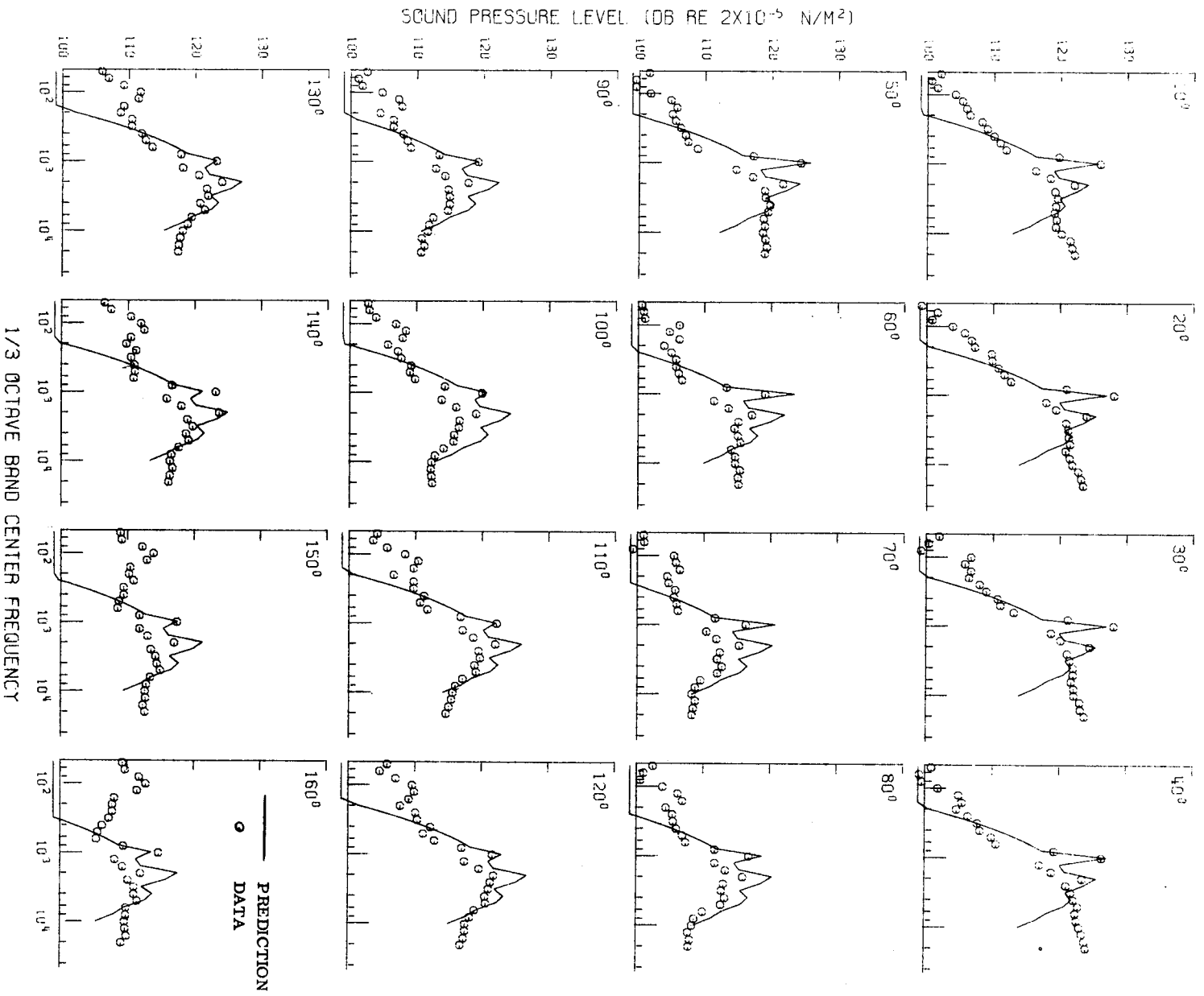
(c) Fan A, configuration 203, 80-percent speed.

Figure 19. - Continued.



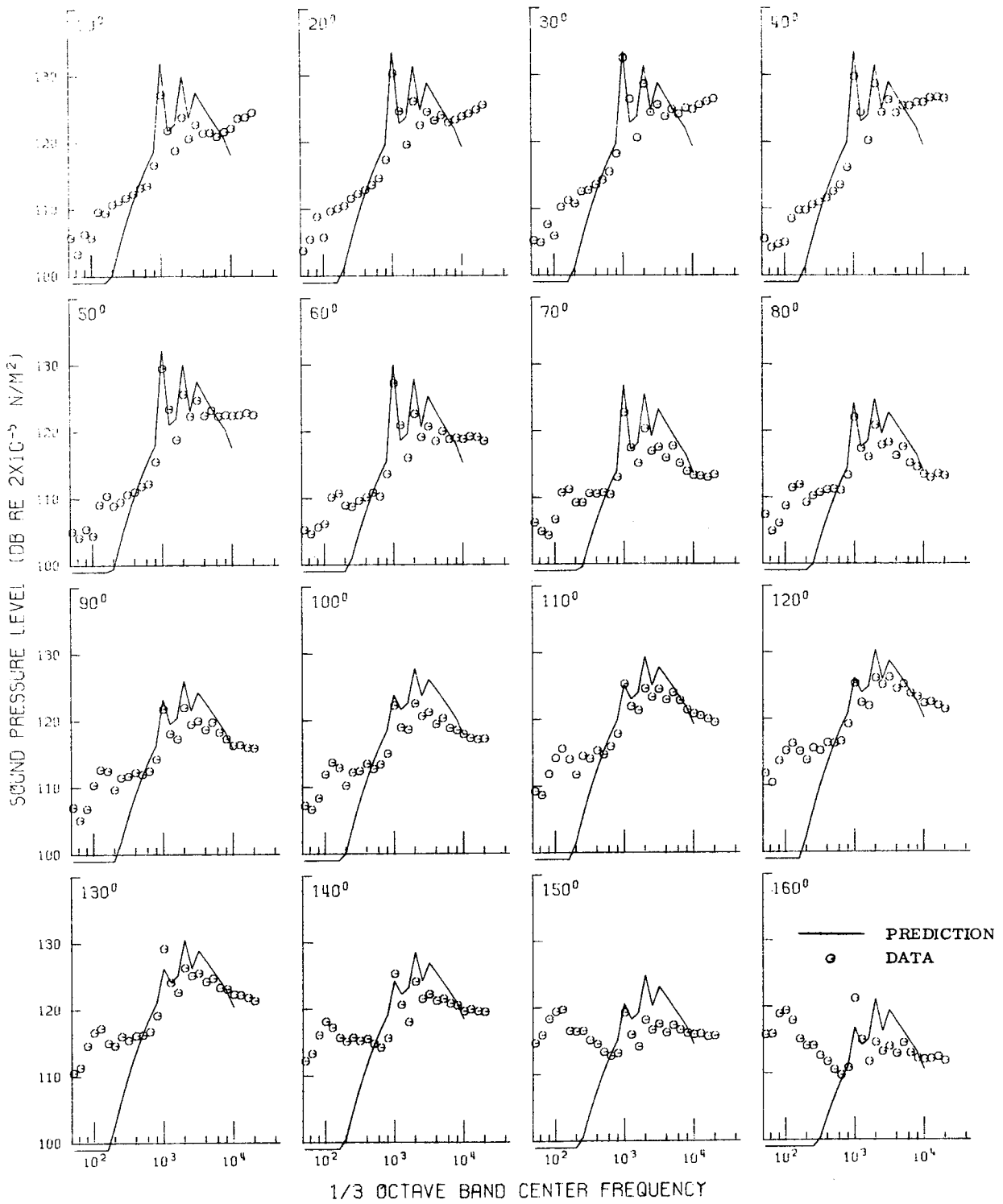
(d) Fan A, configuration 203, 90-percent speed.

Figure 19. - Continued.



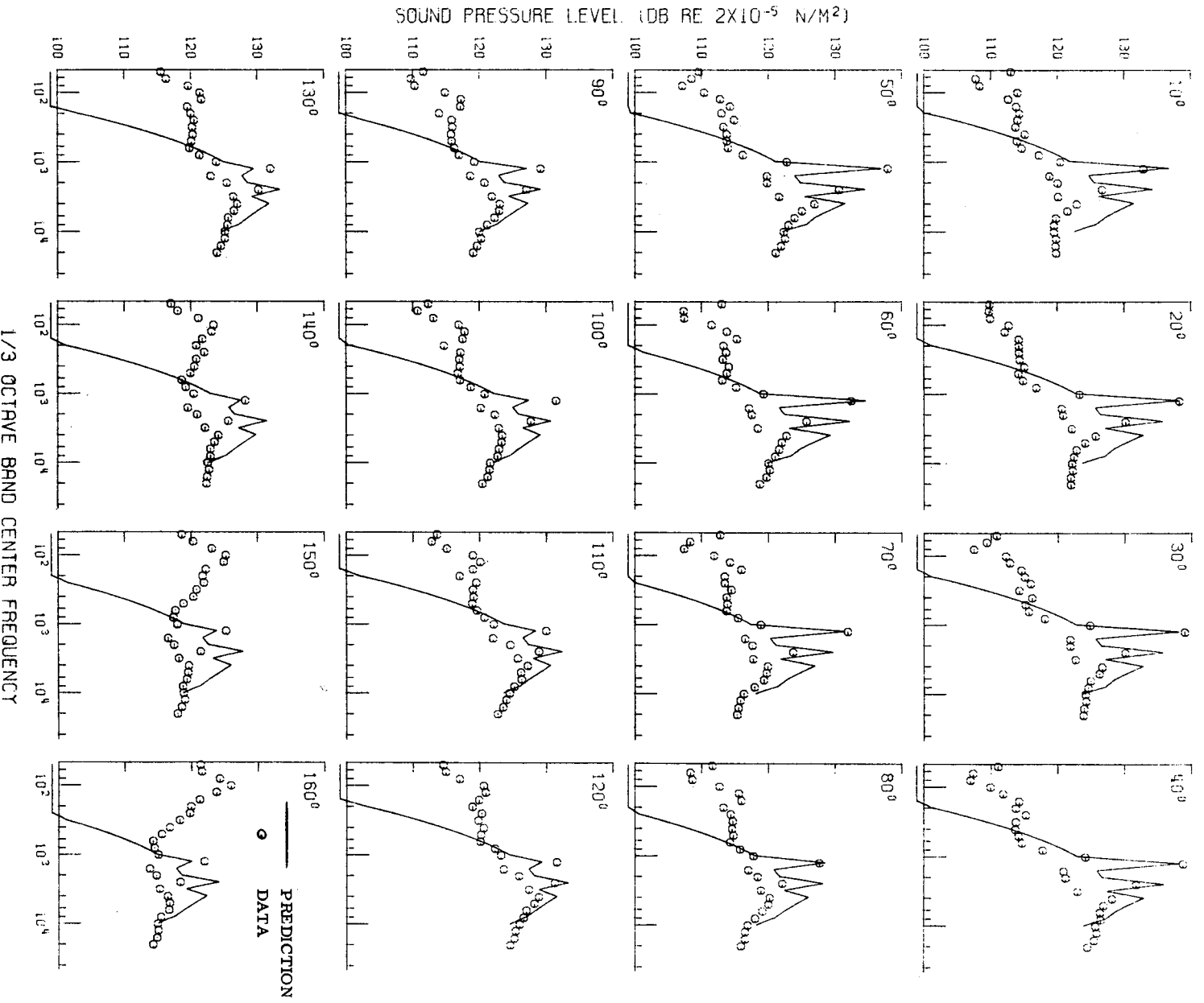
(e) Fan B, configuration 108, 60-percent speed.

Figure 19. - Continued.



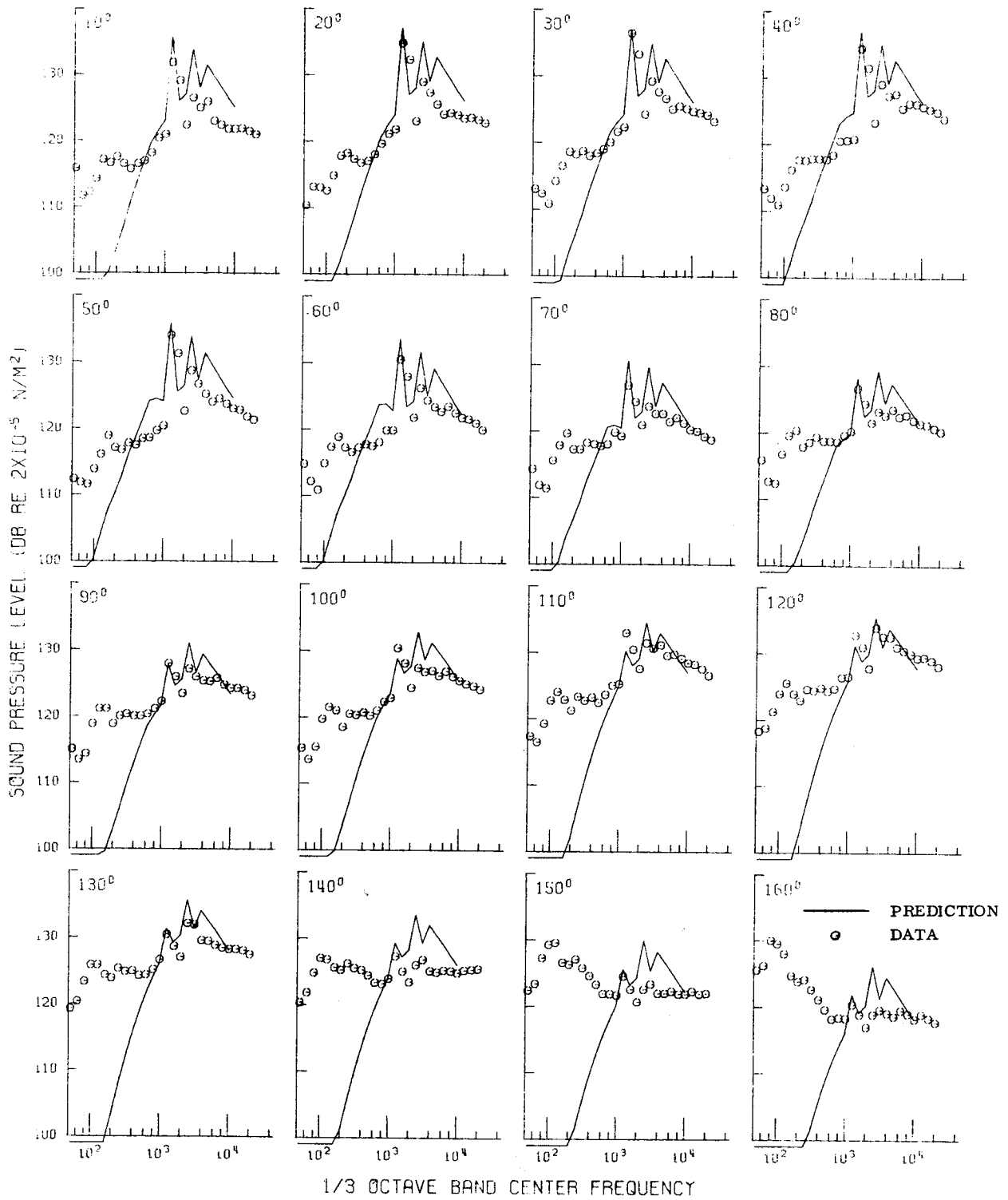
(f) Fan B, configuration 108, 70-percent speed.

Figure 19. - Continued.



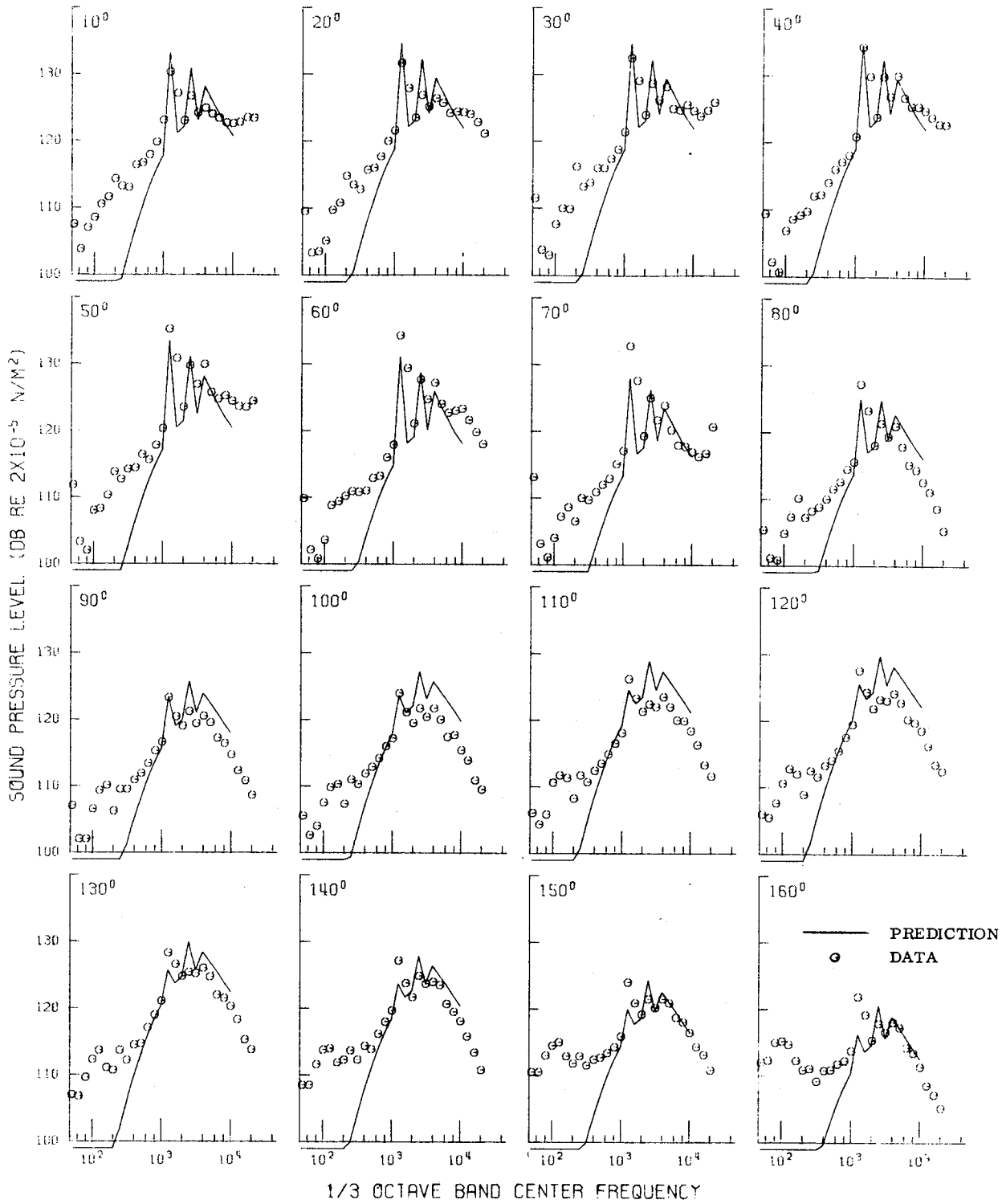
(g) Fan B, configuration 108, 80-percent speed.

Figure 19. - Continued.



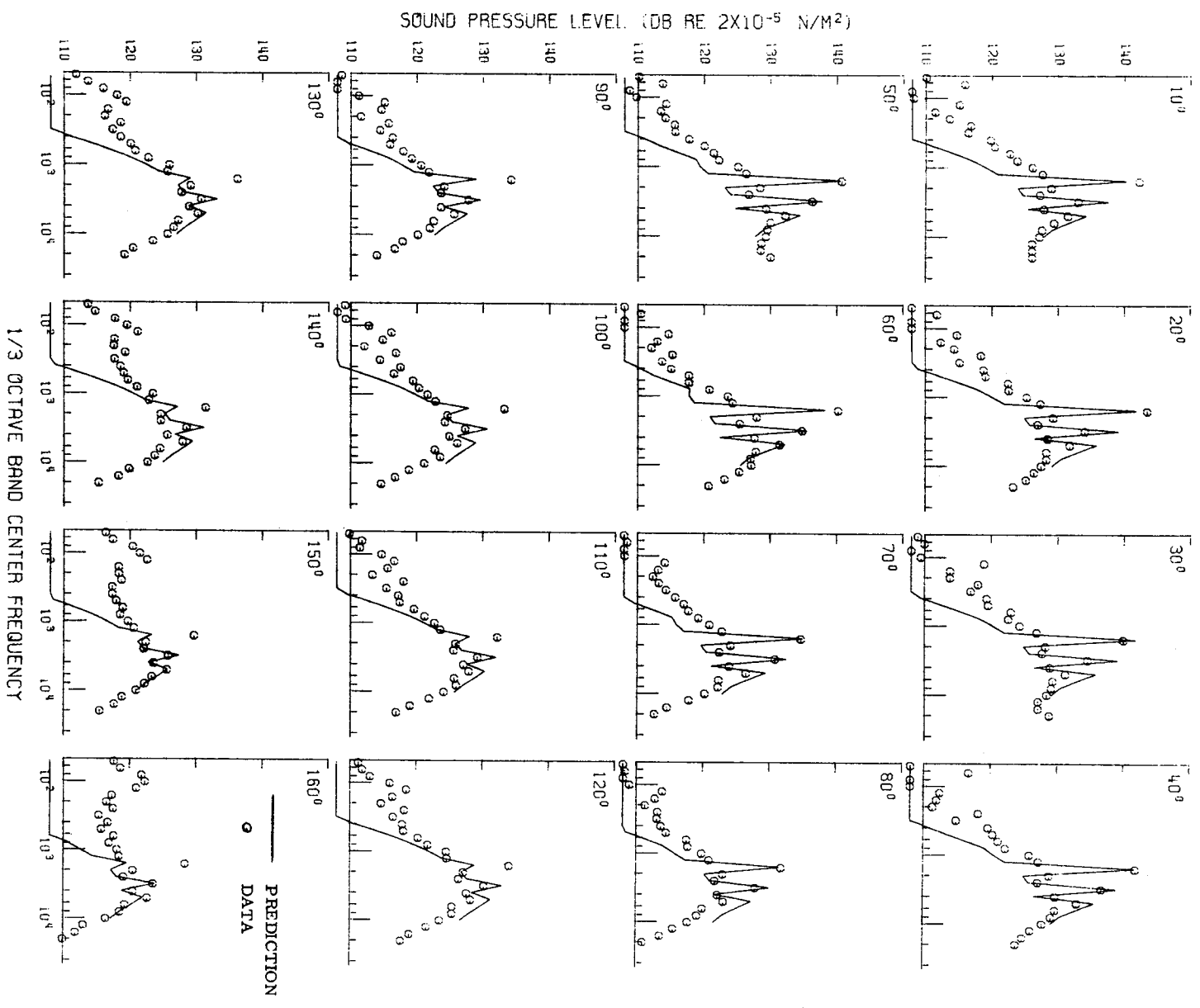
(h) Fan B, configuration 108, 90-percent speed.

Figure 19. - Continued.



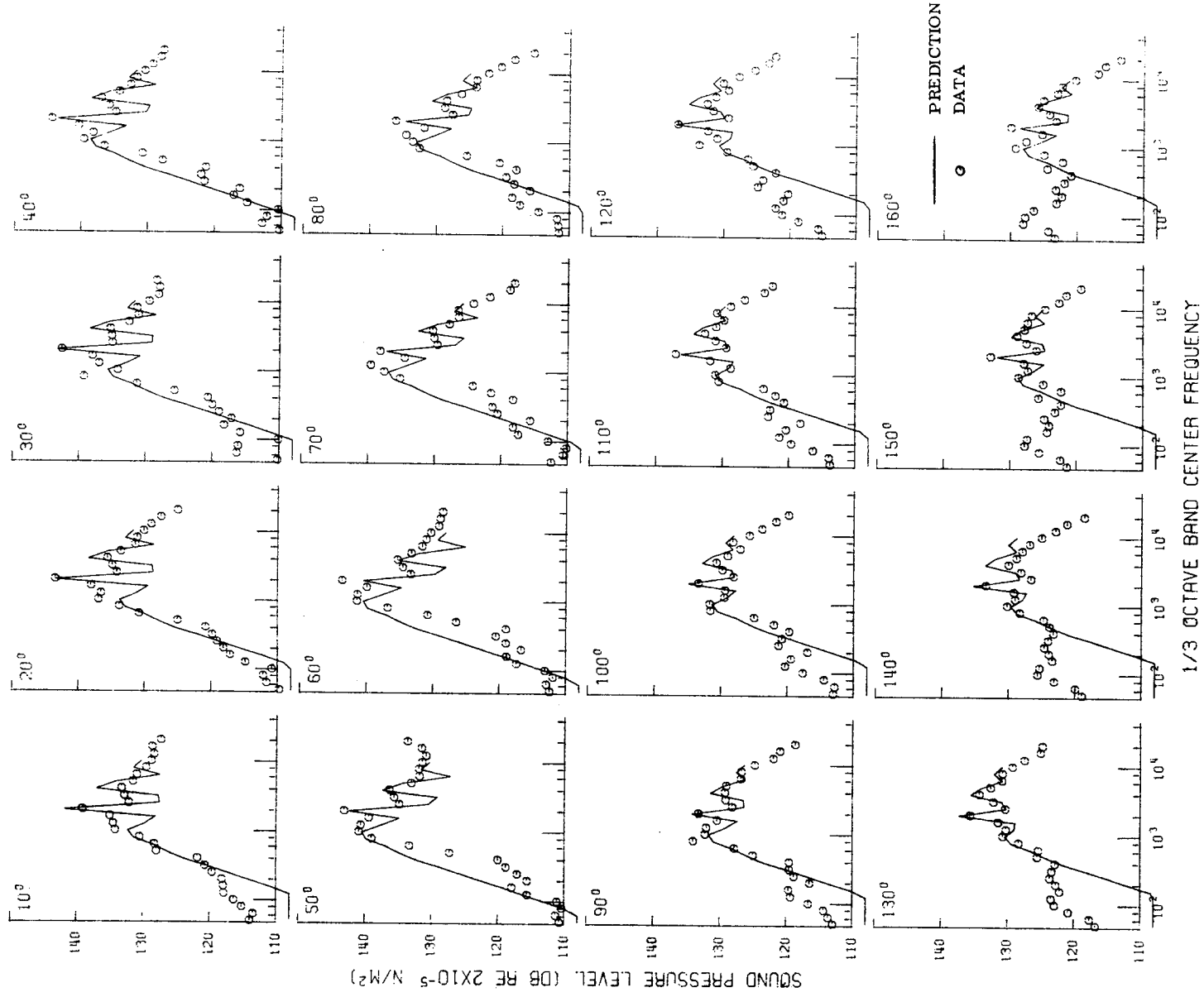
(i) Fan C, configuration 302, 60-percent speed.

Figure 19. - Continued.



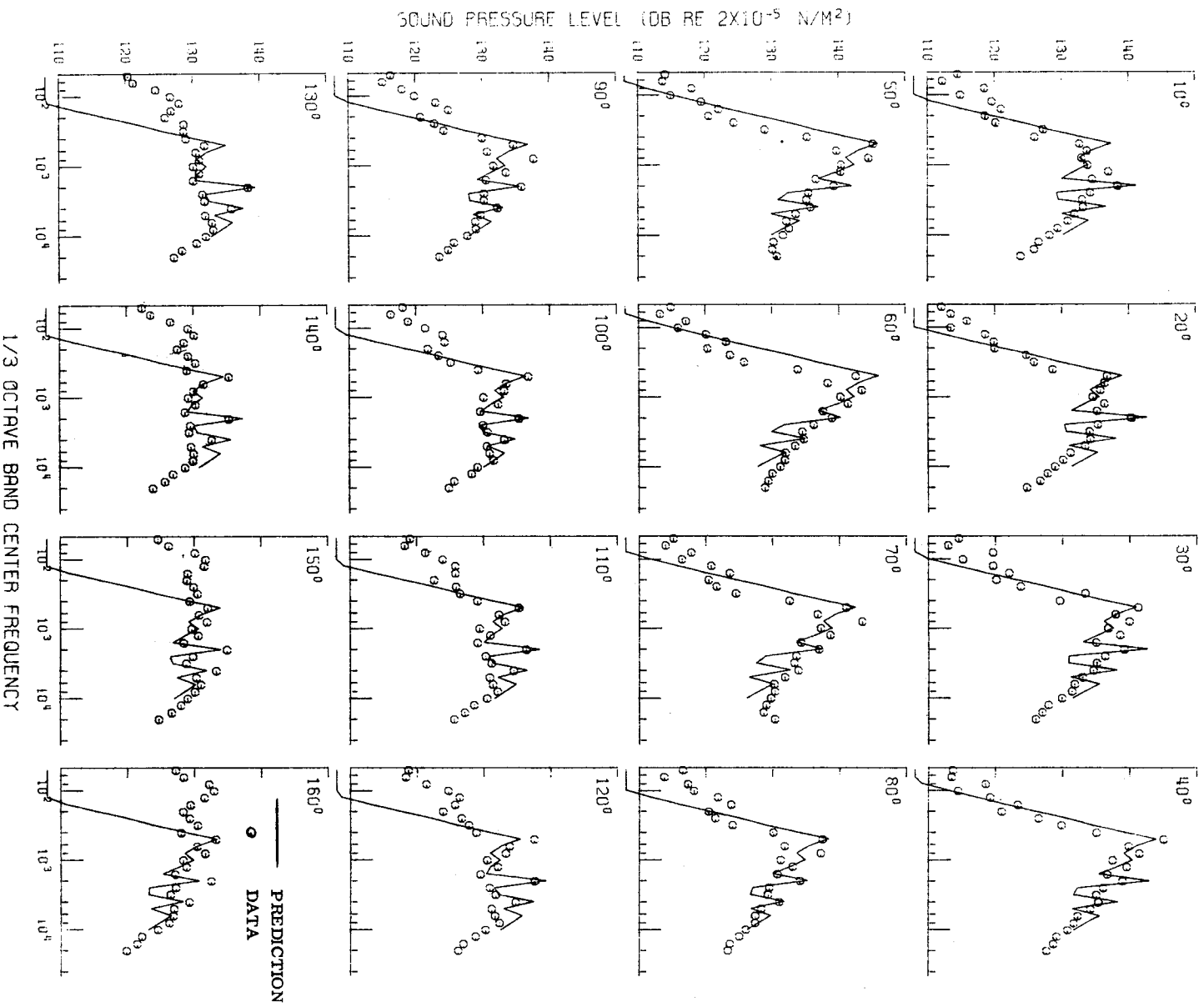
(j) Fan C, configuration 302, 70-percent speed.

Figure 19. - Continued.



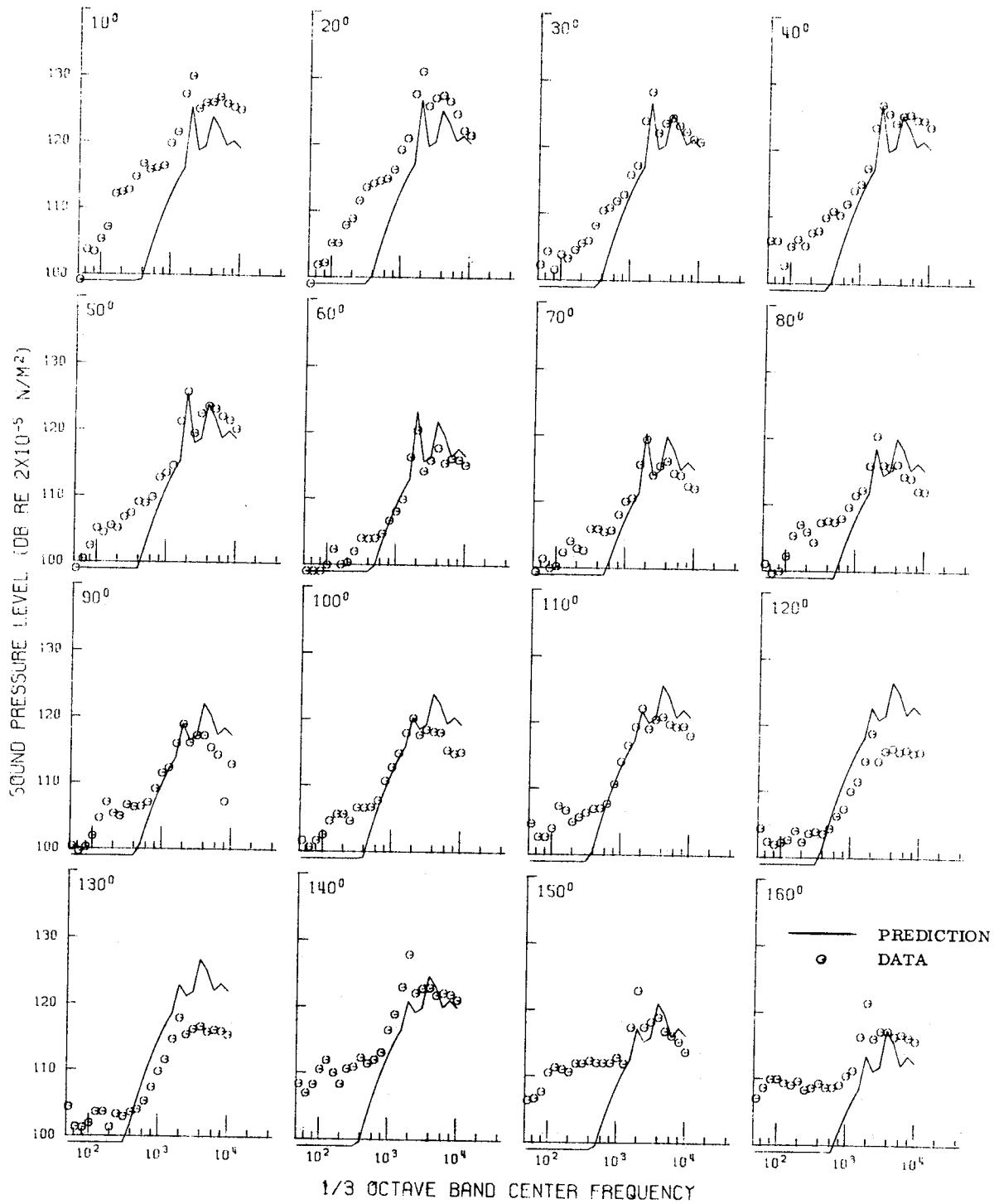
(k) Fan C, configuration 302, 80-percent speed.

Figure 19. - Continued.



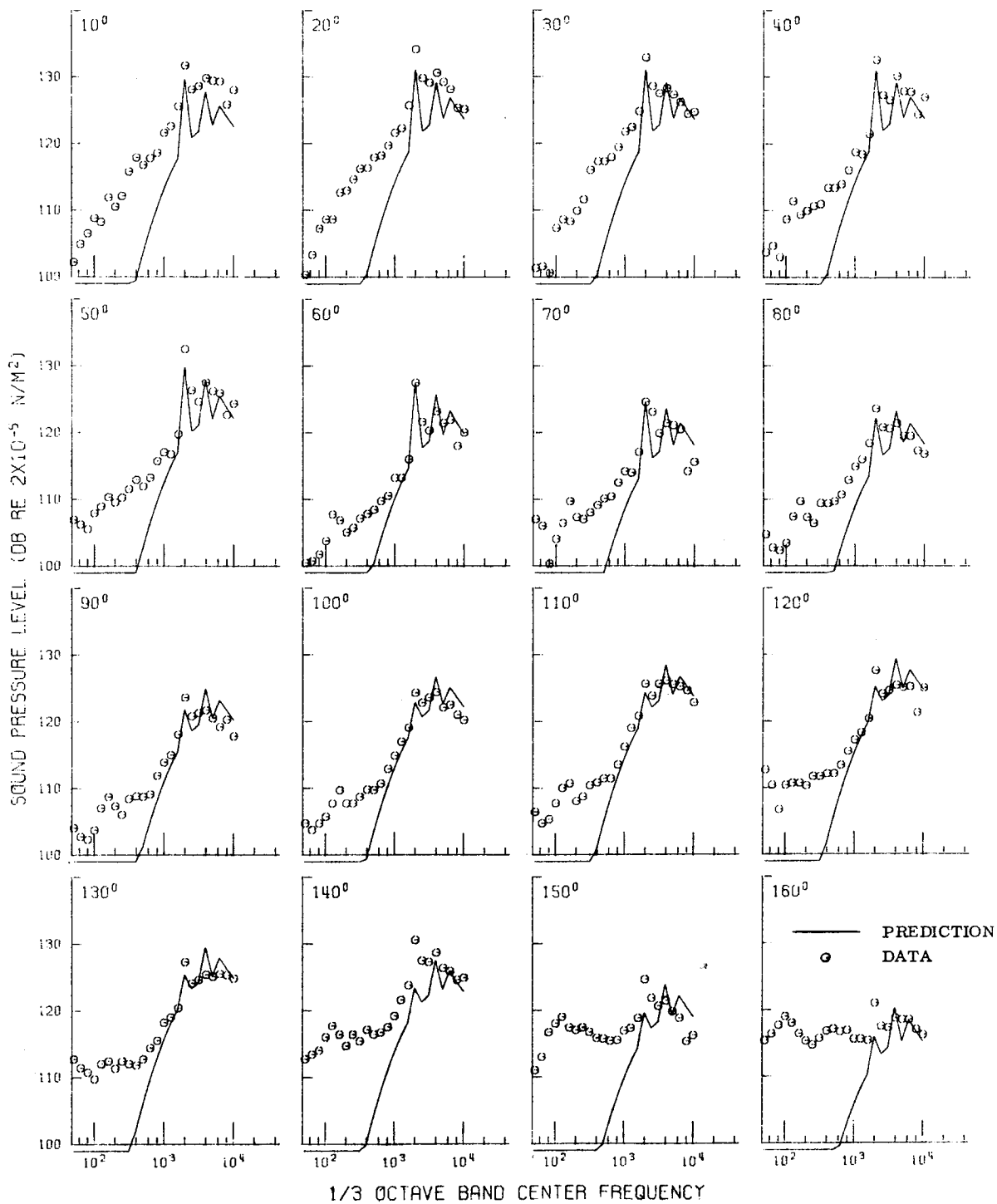
(1) Fan C, configuration 302, 90-percent speed.

Figure 19. - Continued.



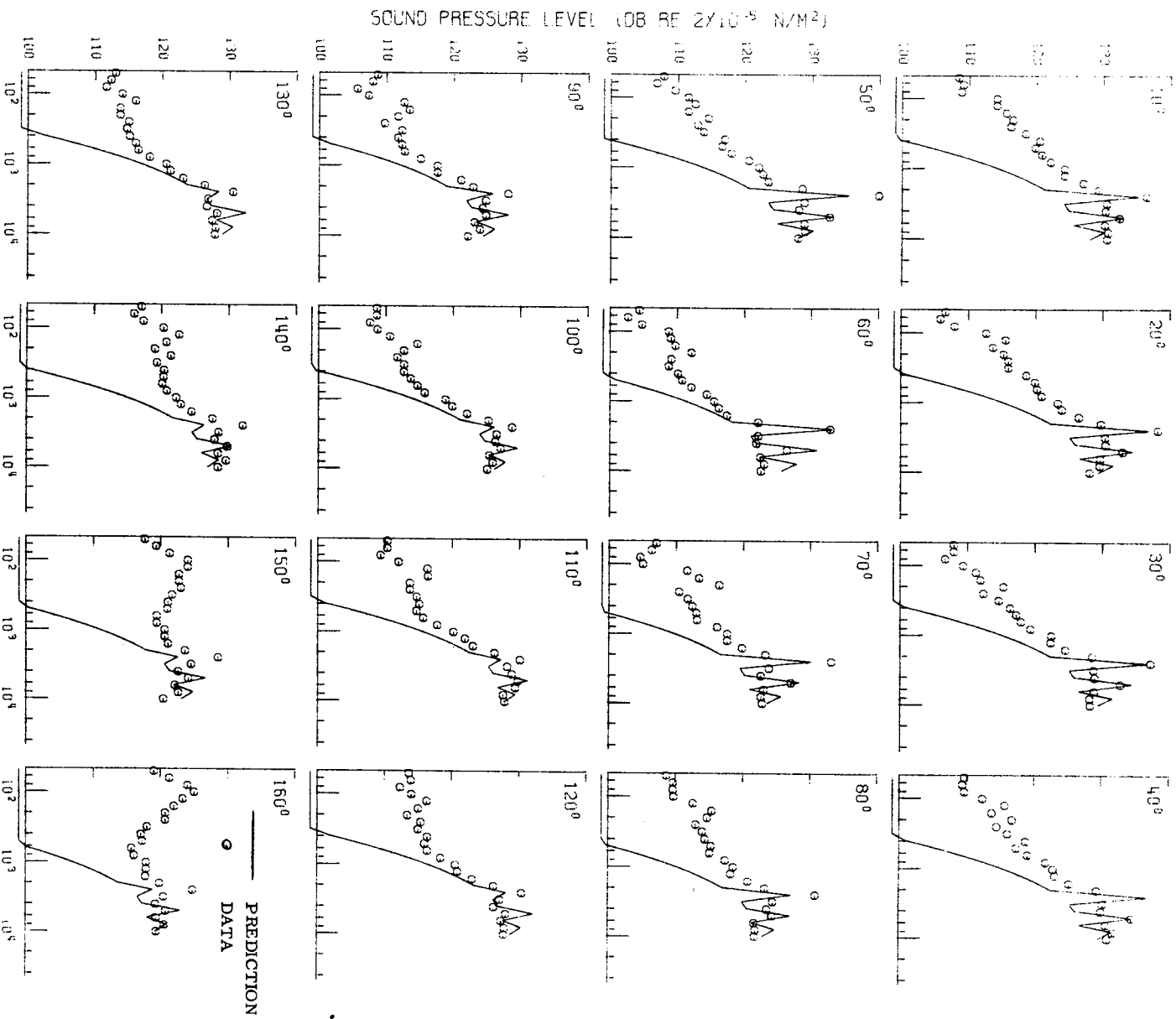
(m) Fan QF-1, configuration 3, 60-percent speed.

Figure 19. - Continued.



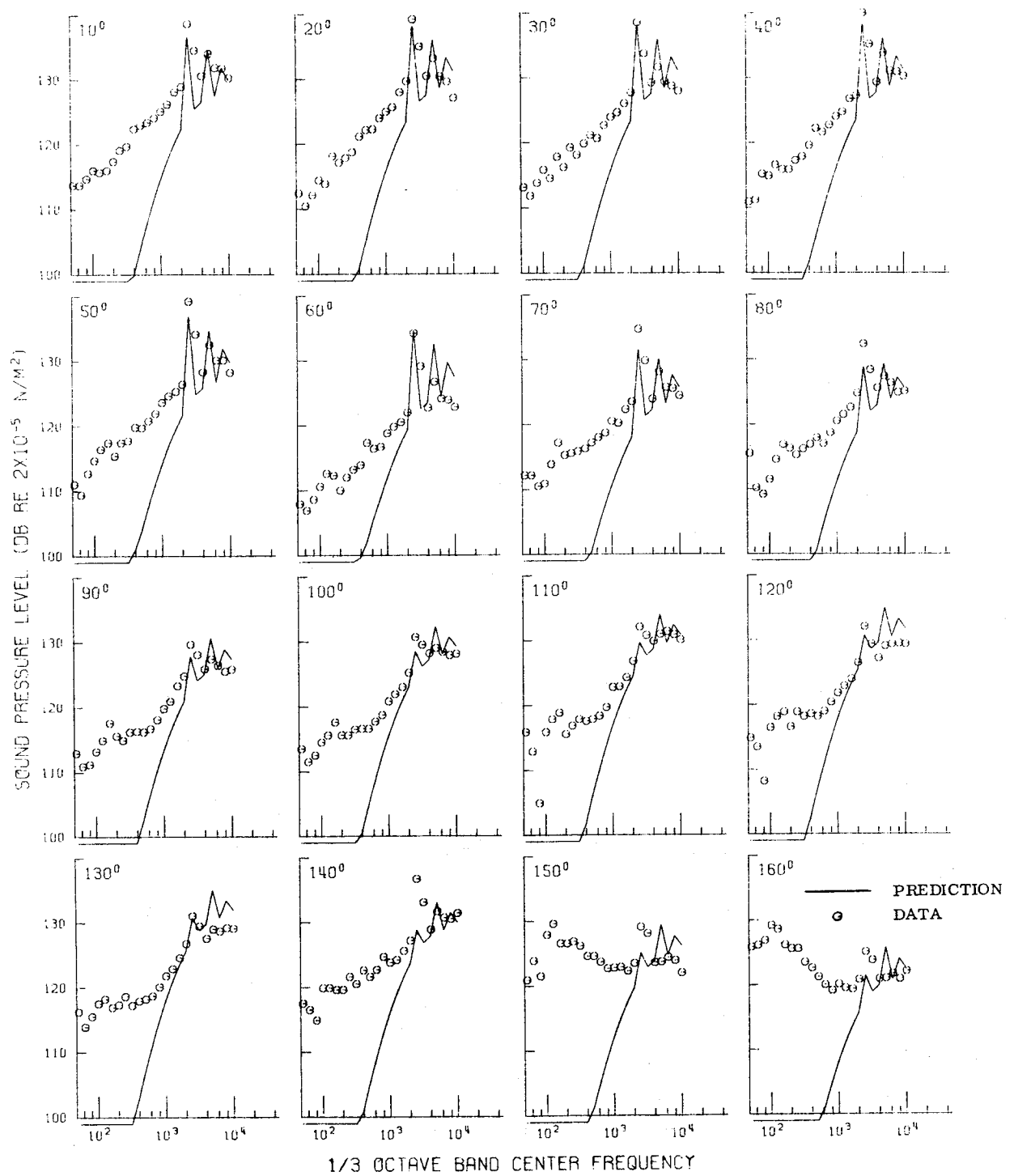
(n) Fan QF-1, configuration 3, 70-percent speed.

Figure 19. - Continued.



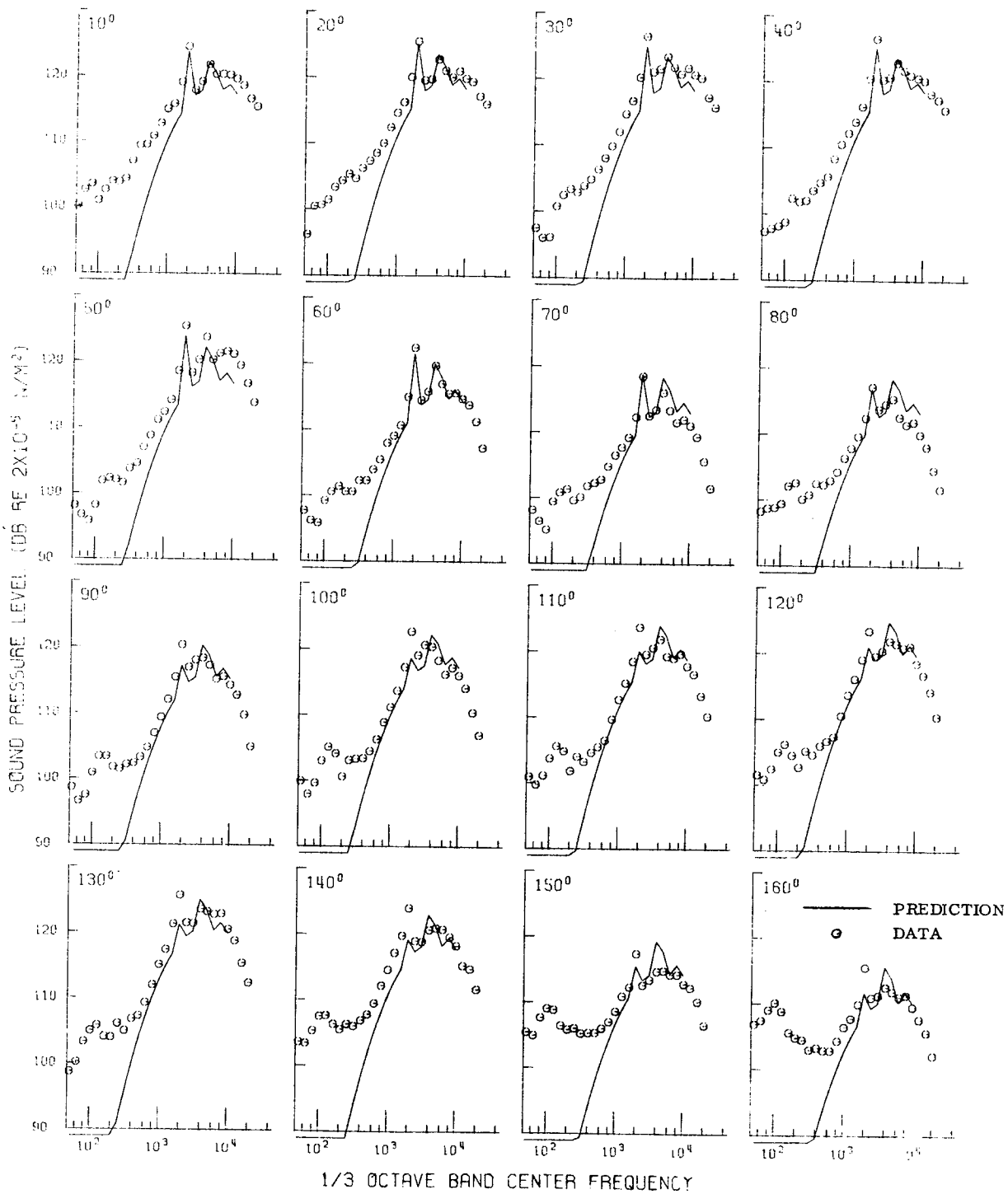
(o) Fan QF-1, configuration 3, 80-percent speed.

Figure 19. - Continued.



(p) Fan QF-1, configuration 3, 90-percent speed.

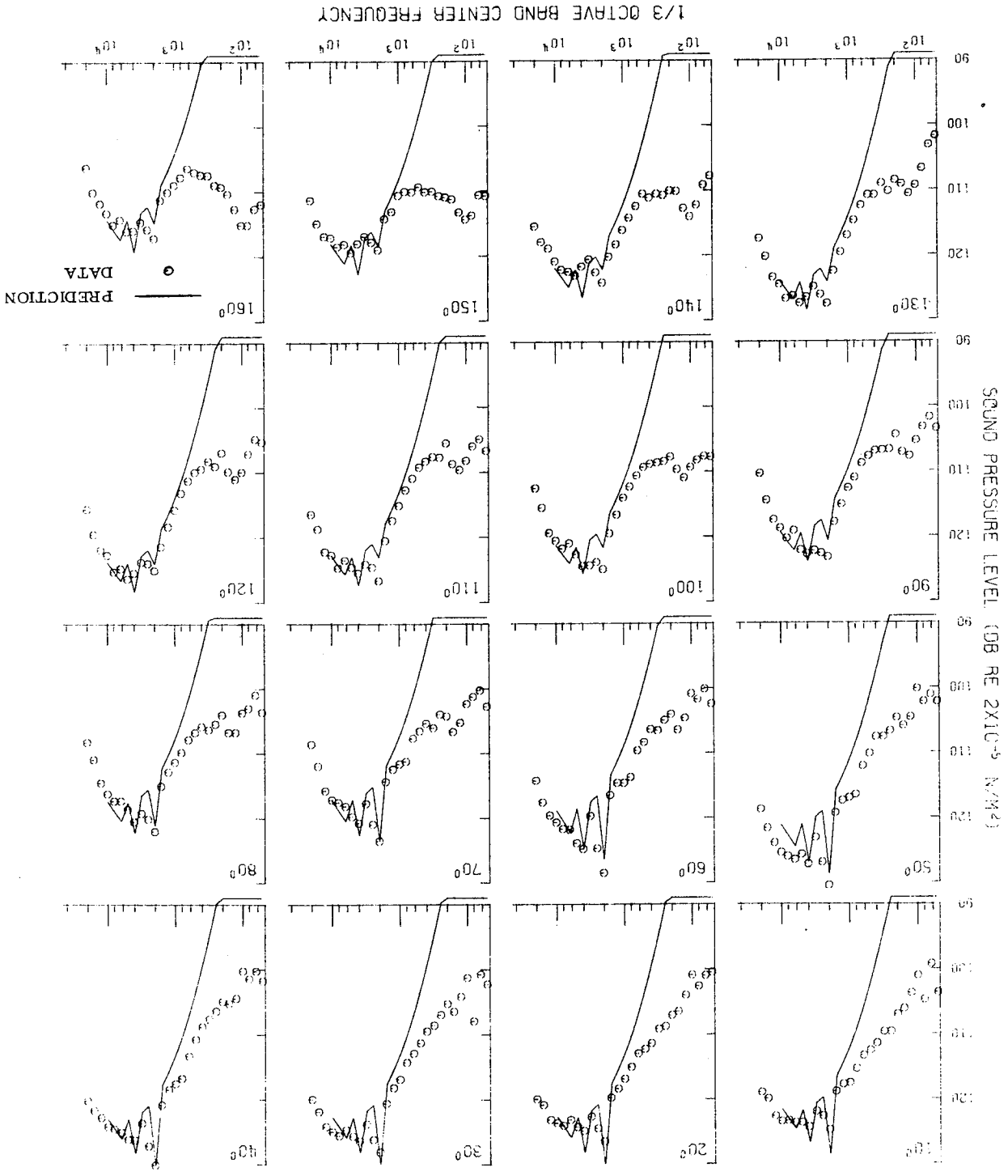
Figure 19. - Continued.

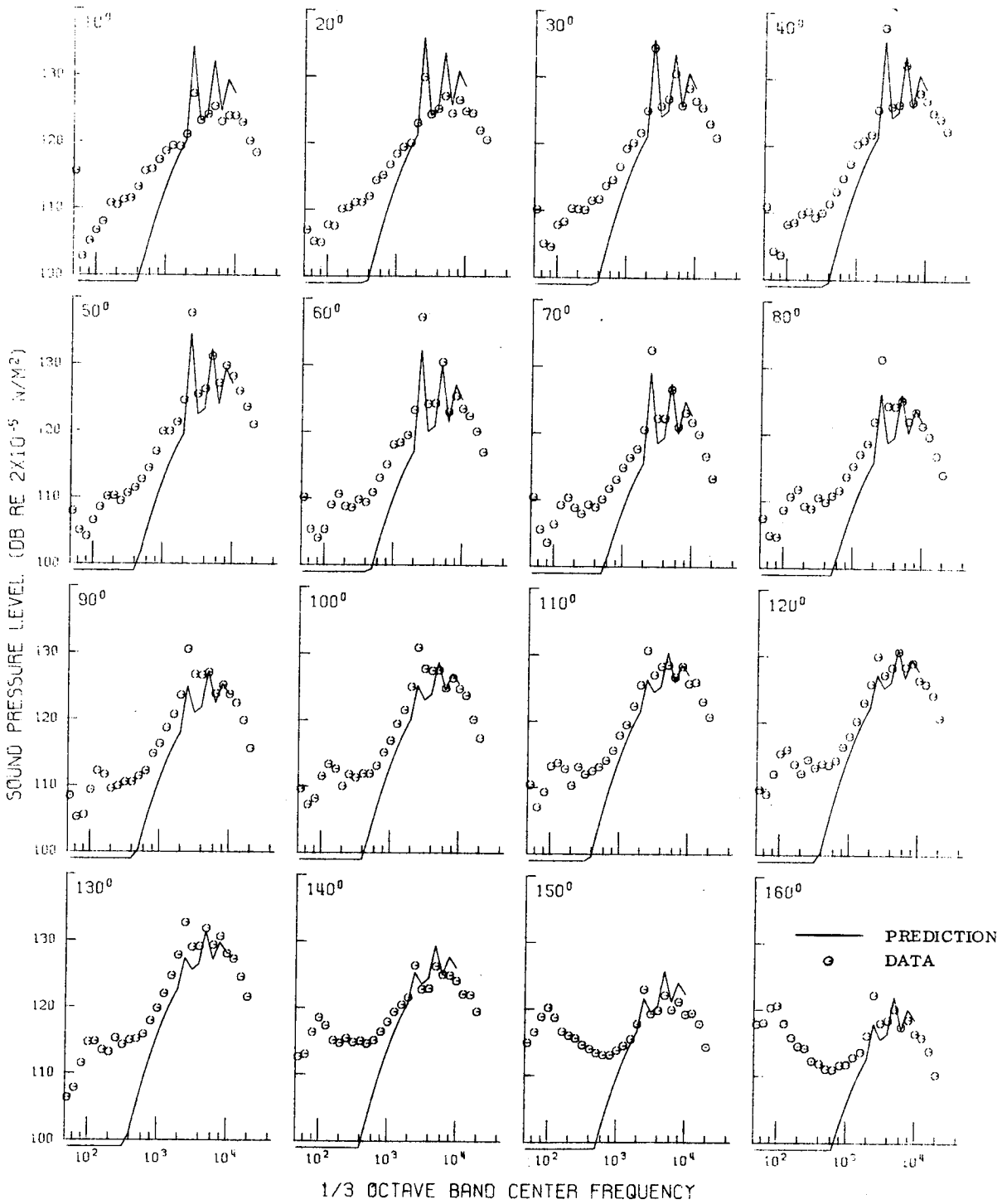


(q) Fan QF-3, configuration 27, 60-percent speed.

Figure 19. - Continued.

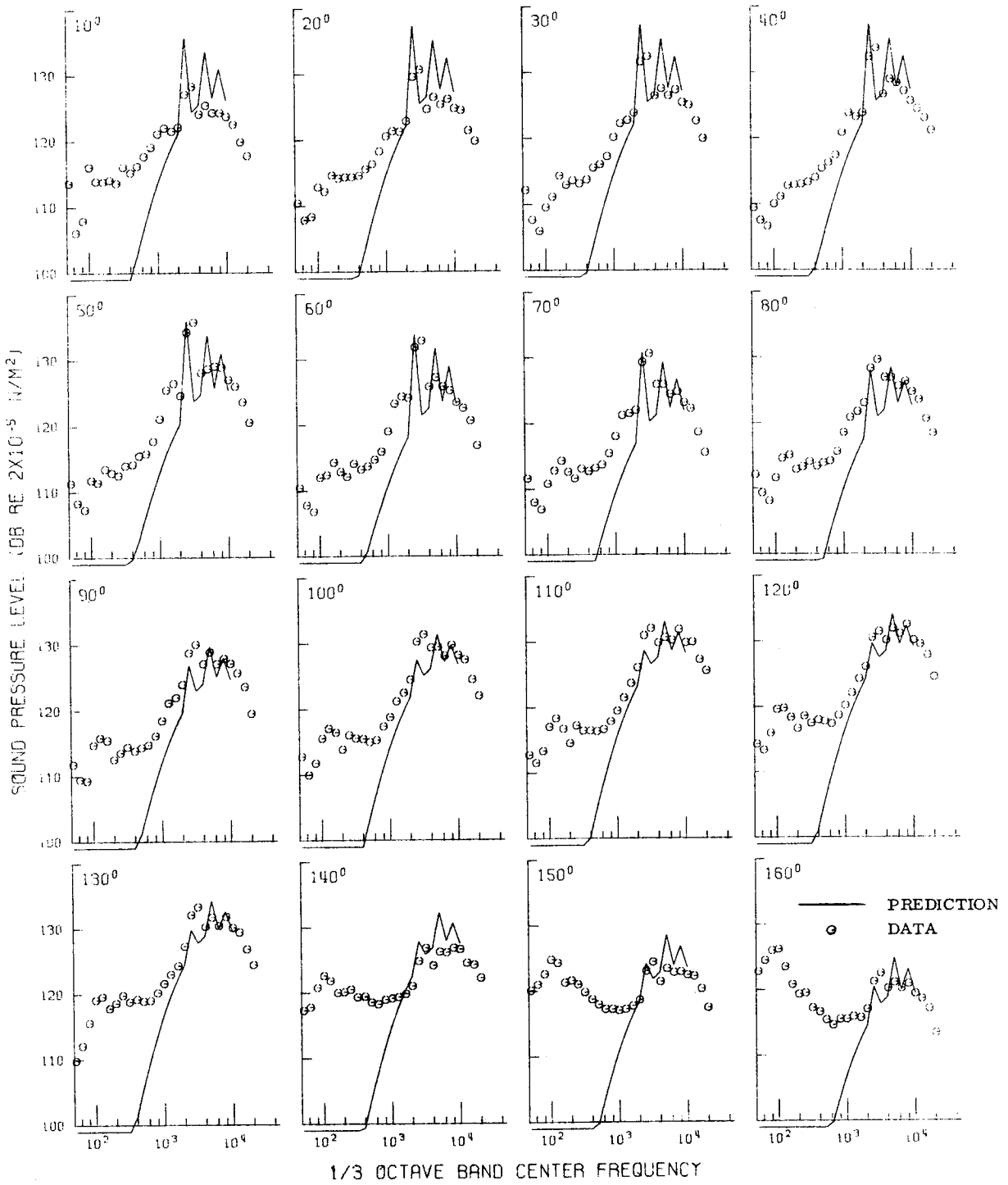
(r) Fan QF-3, configuration 27, 70-percent speed.
Figure 19. - Continued.





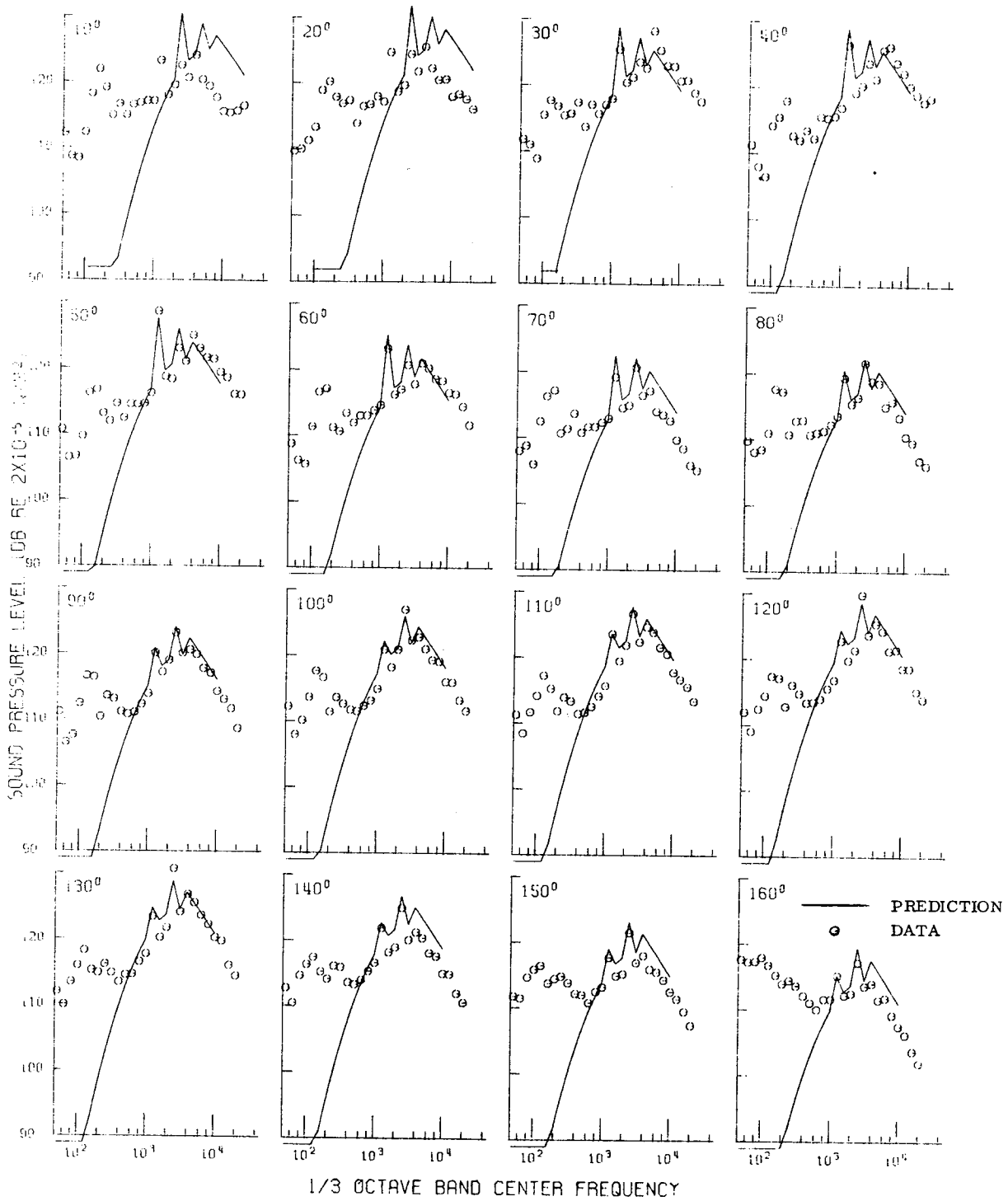
(s) Fan QF-3, configuration 27, 80-percent speed.

Figure 19. - Continued.



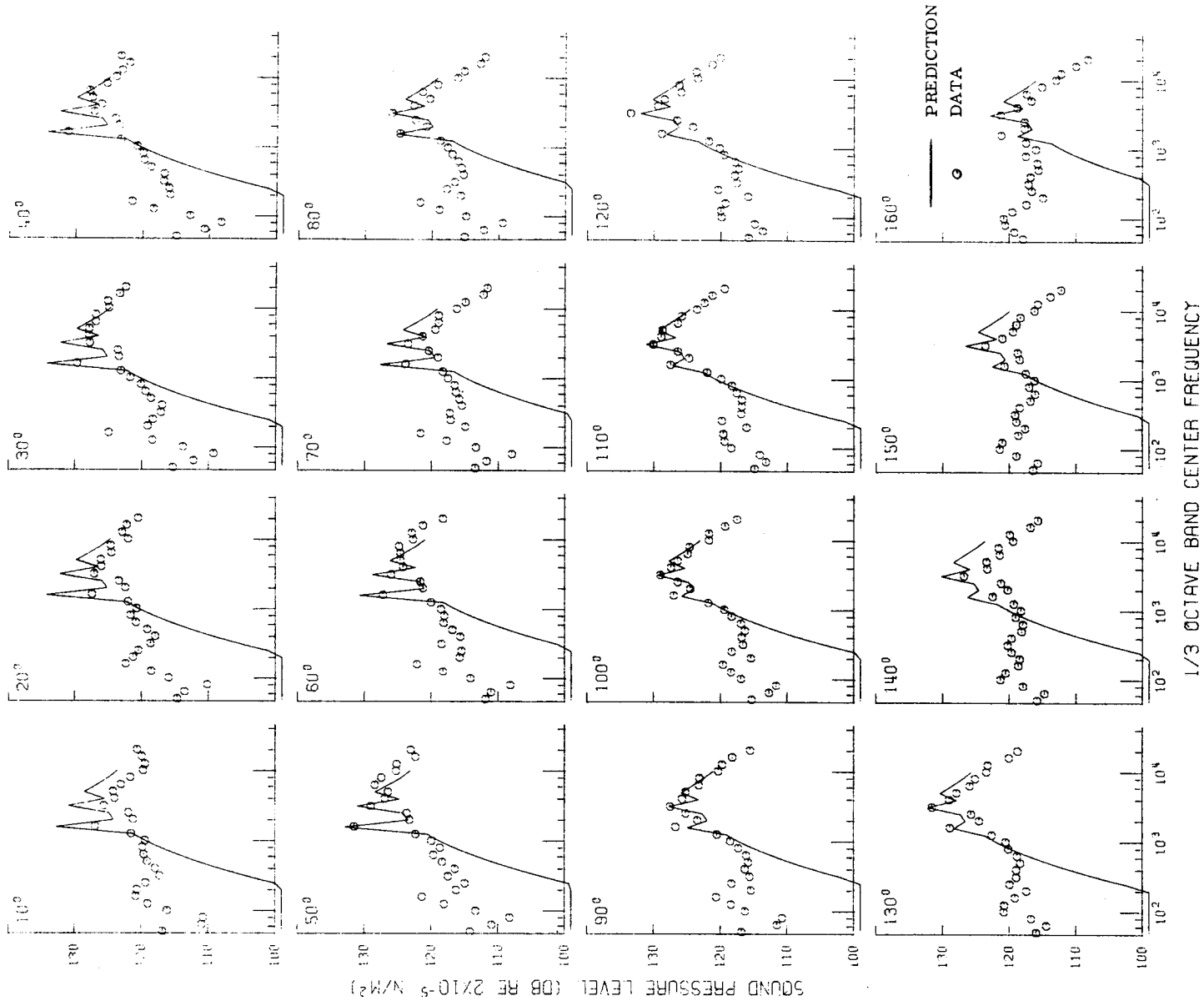
(t) Fan QF-3, configuration 27, 90-percent speed.

Figure 19. - Continued.



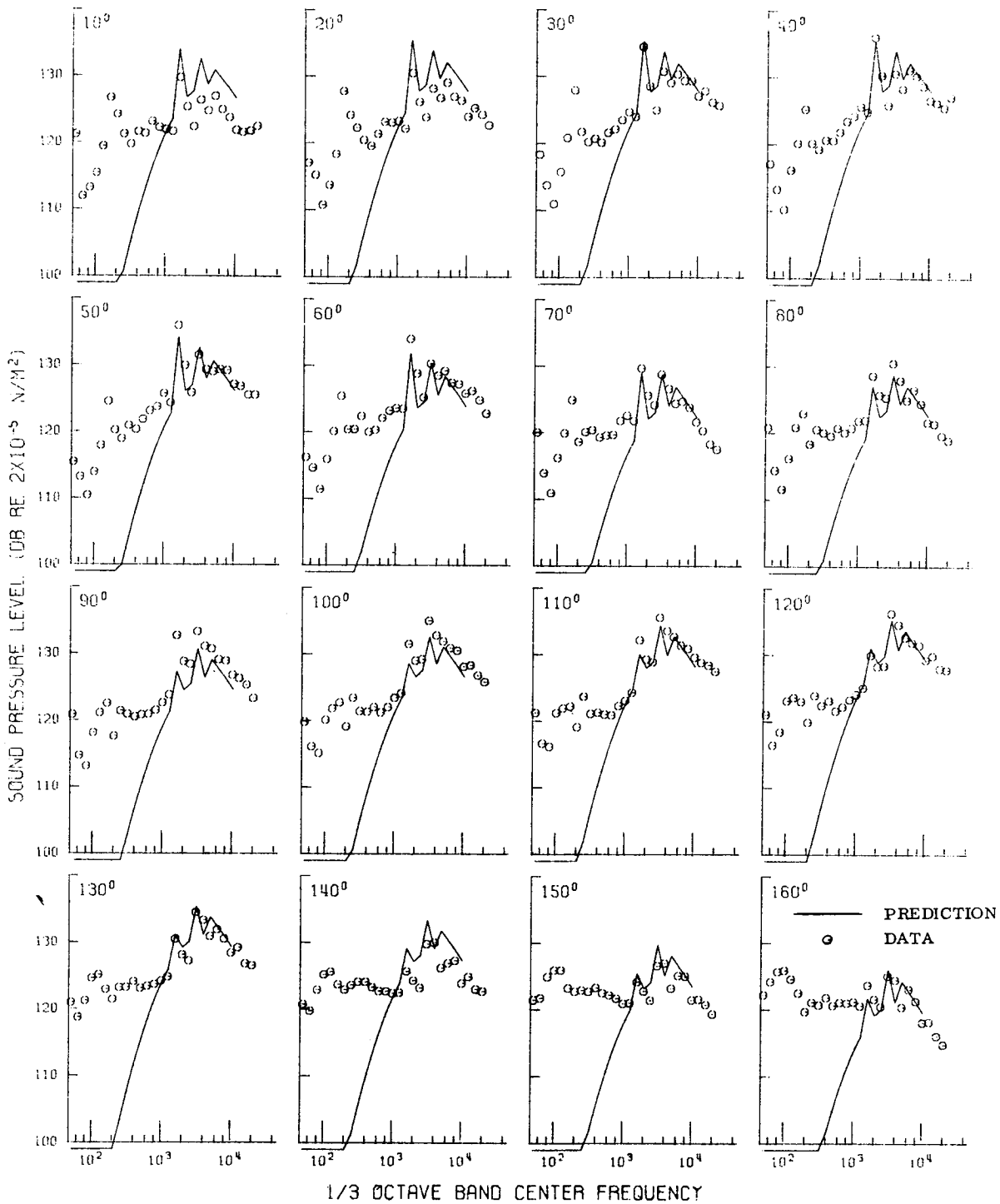
(u) Fan QF-5, configuration 43, 60-percent speed.

Figure 19. - Continued.



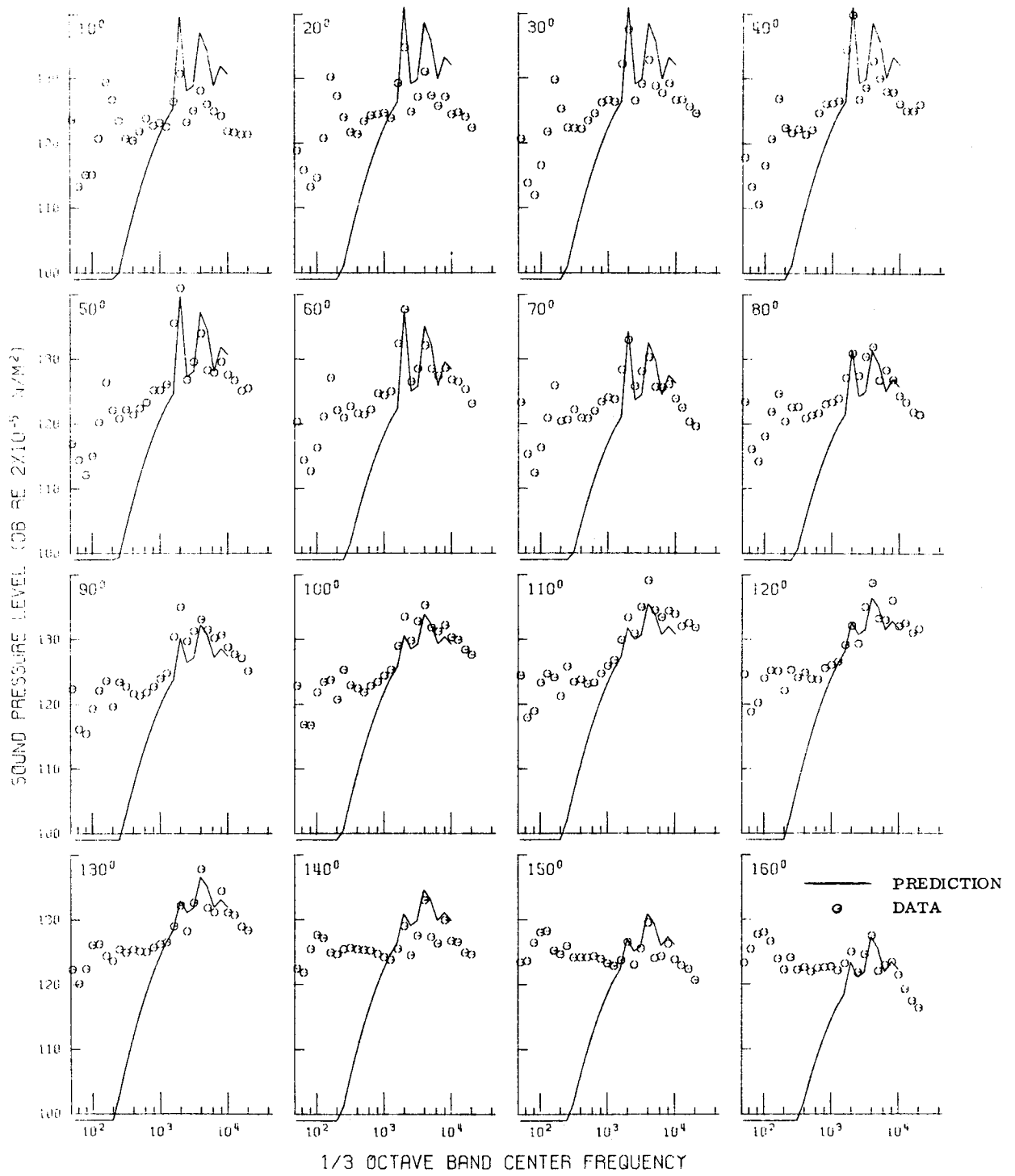
(v) Fan QF-5, configuration 43, 70-percent speed.

Figure 19. - Continued.



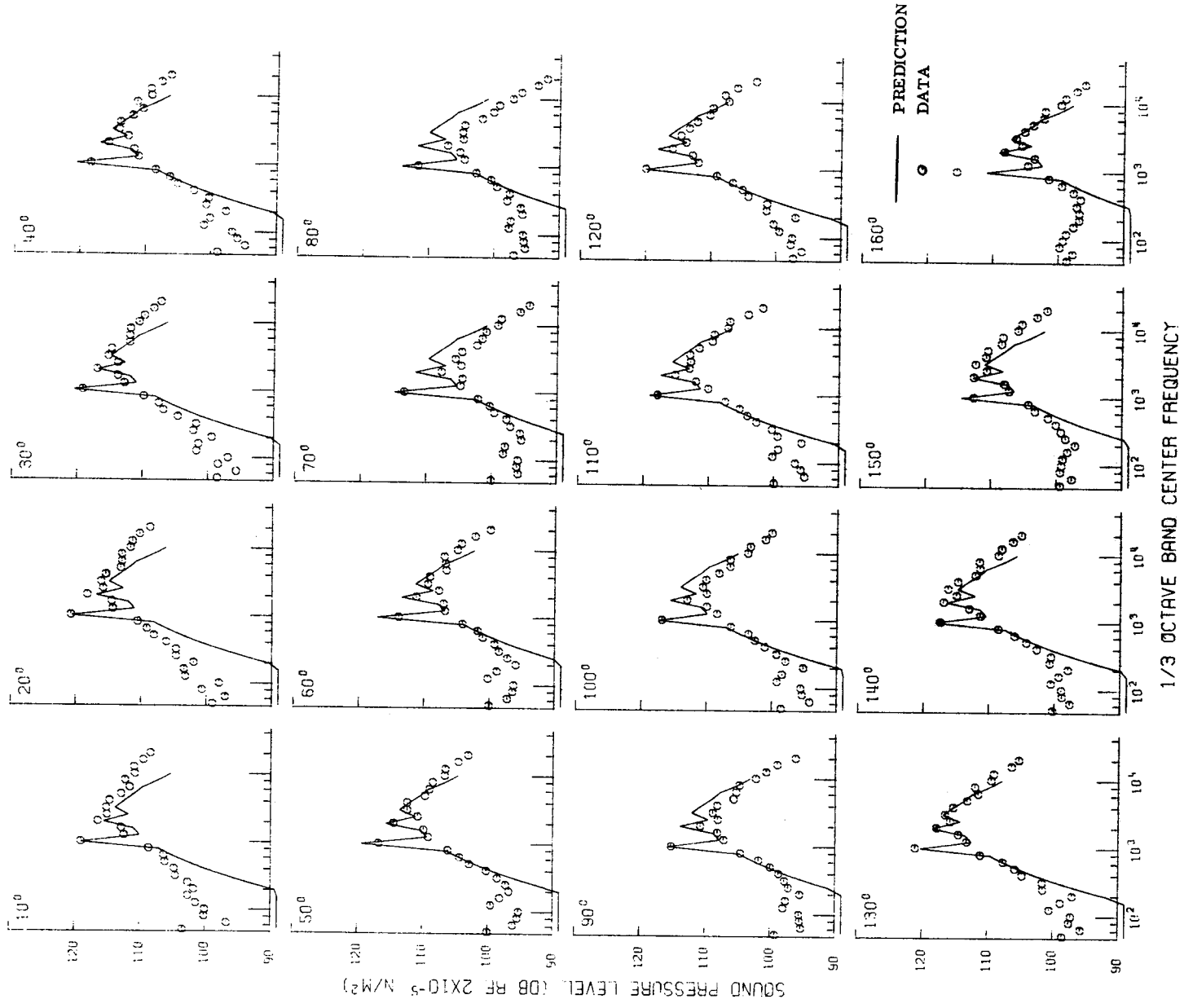
(w) Fan QF-5, configuration 43, 80-percent speed.

Figure 19. - Continued.



(x) Fan QF-5, configuration 43, 85-percent speed.

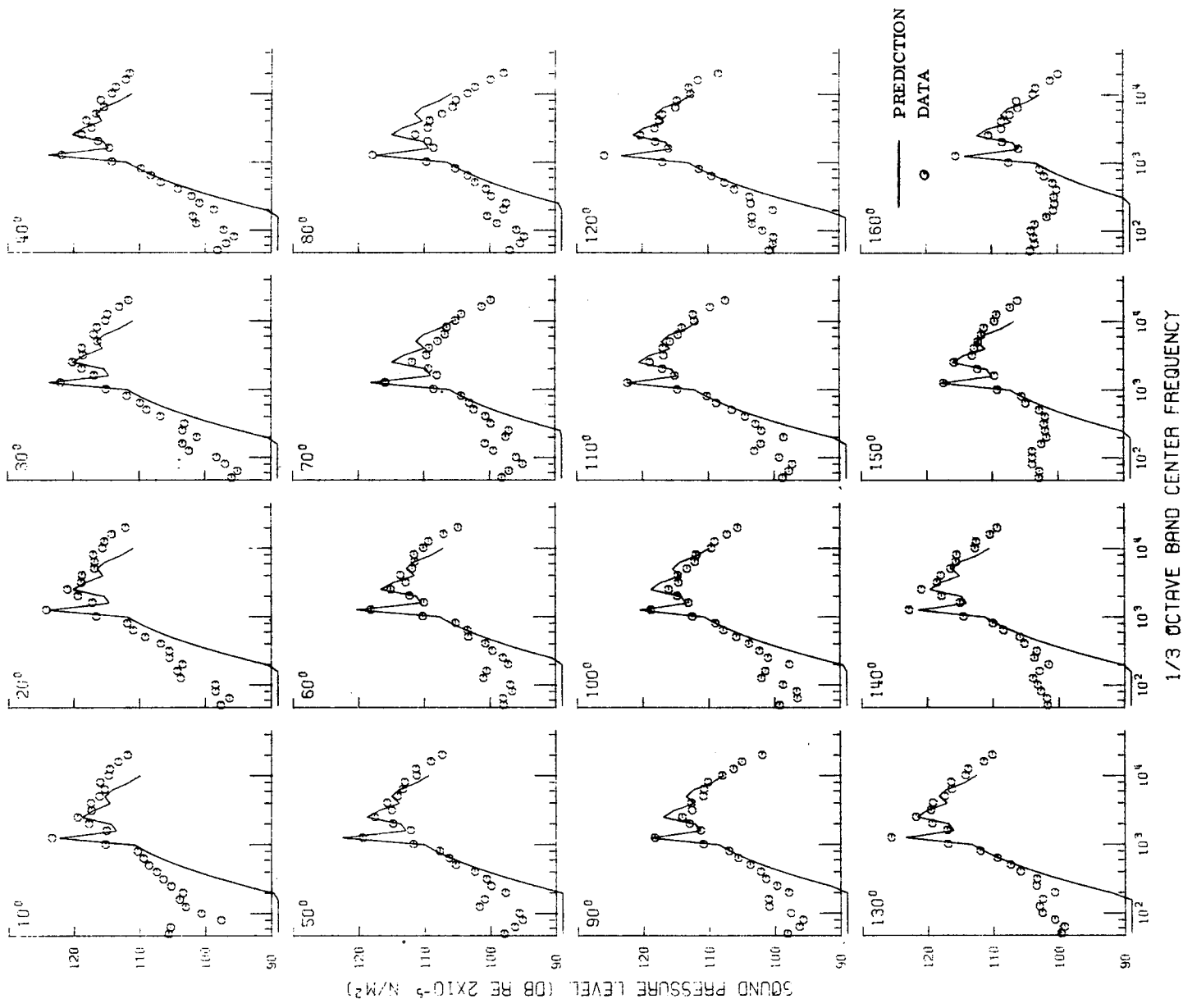
Figure 19. - Continued.



1/3 OCTAVE BAND CENTER FREQUENCY

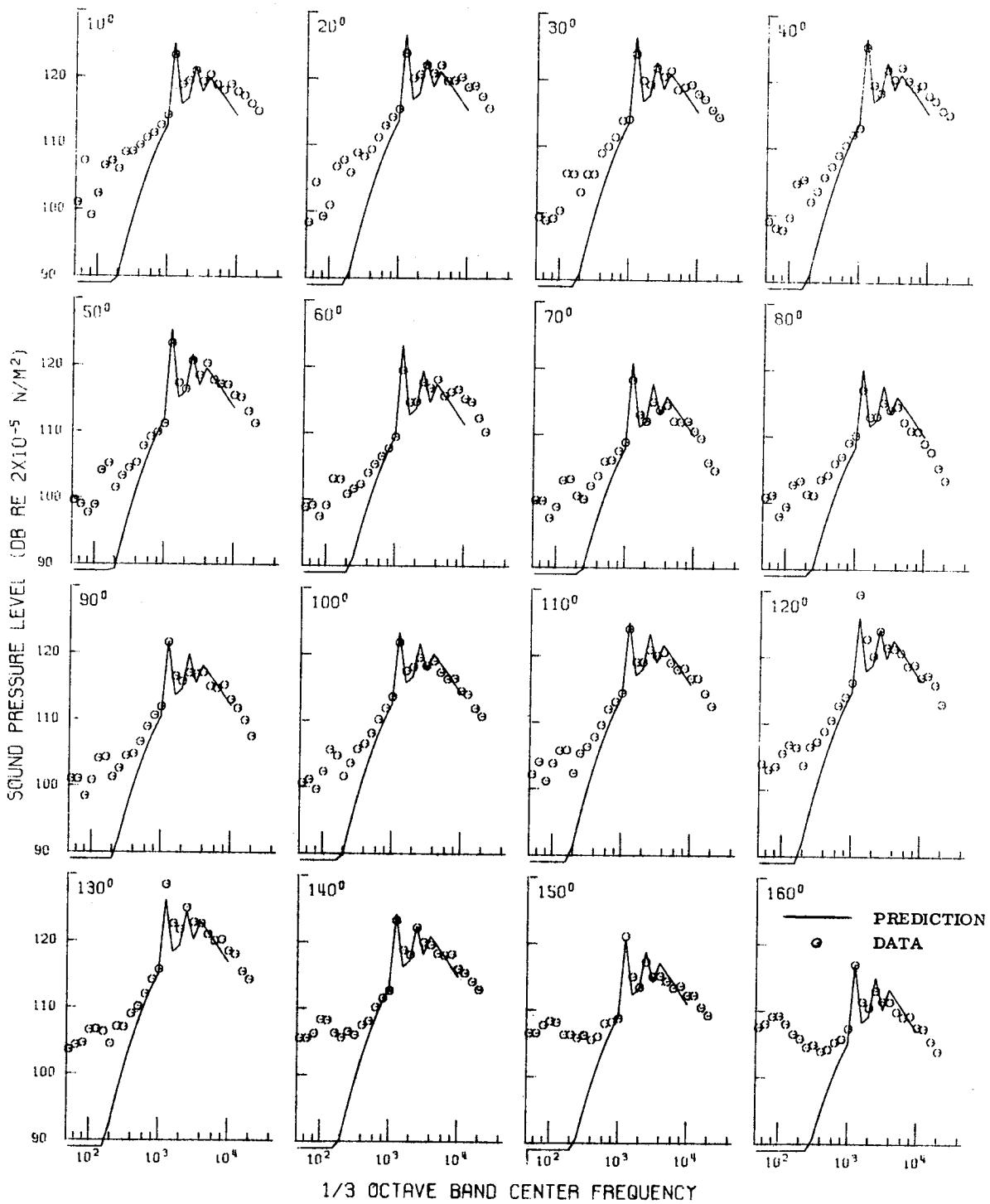
(Y) Fan QF-6, configuration 45, 60-percent speed.

Figure 19. - Continued.



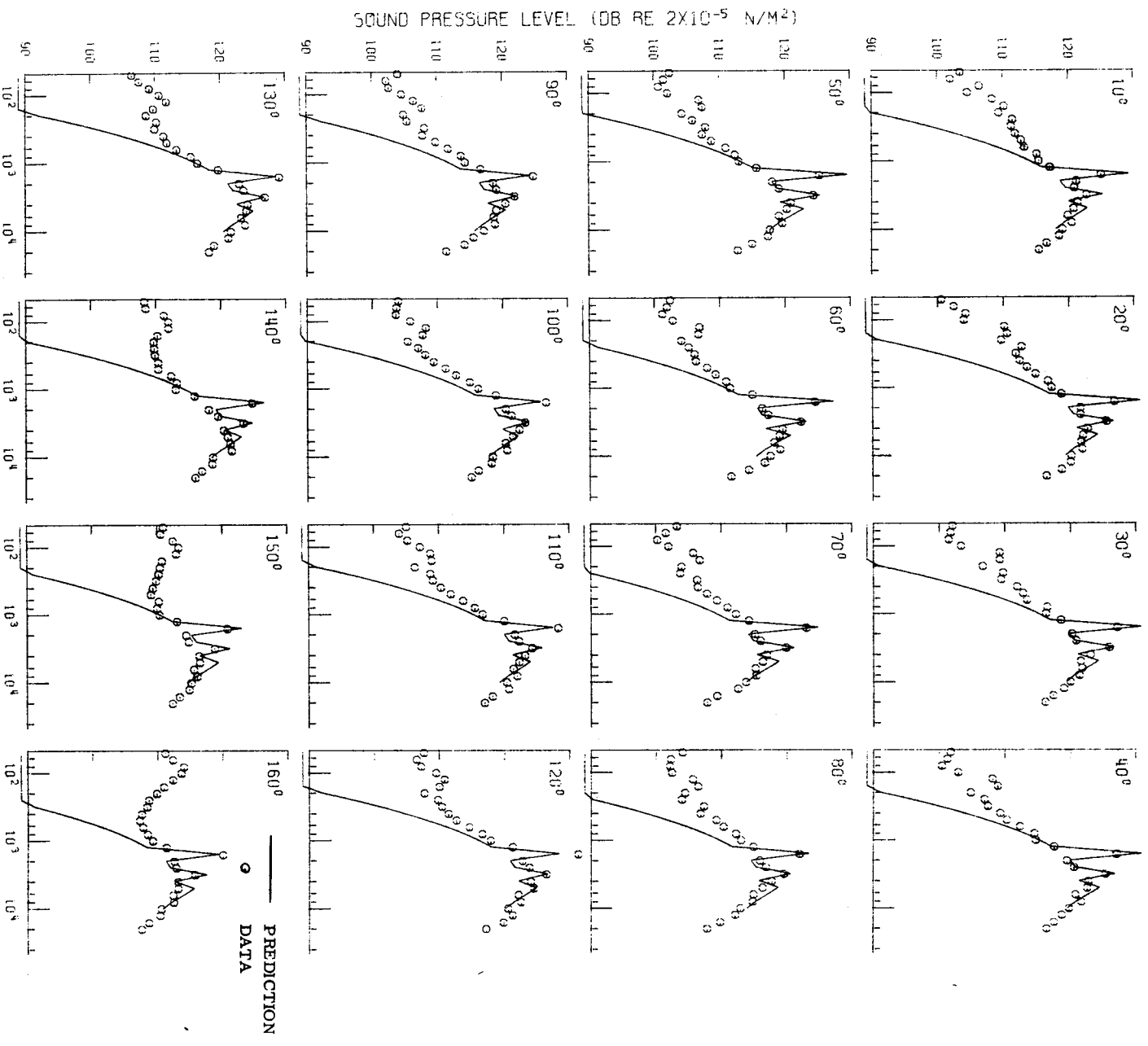
(z) Fan QF-6, configuration 45, 70-percent speed.

Figure 19. - Continued.



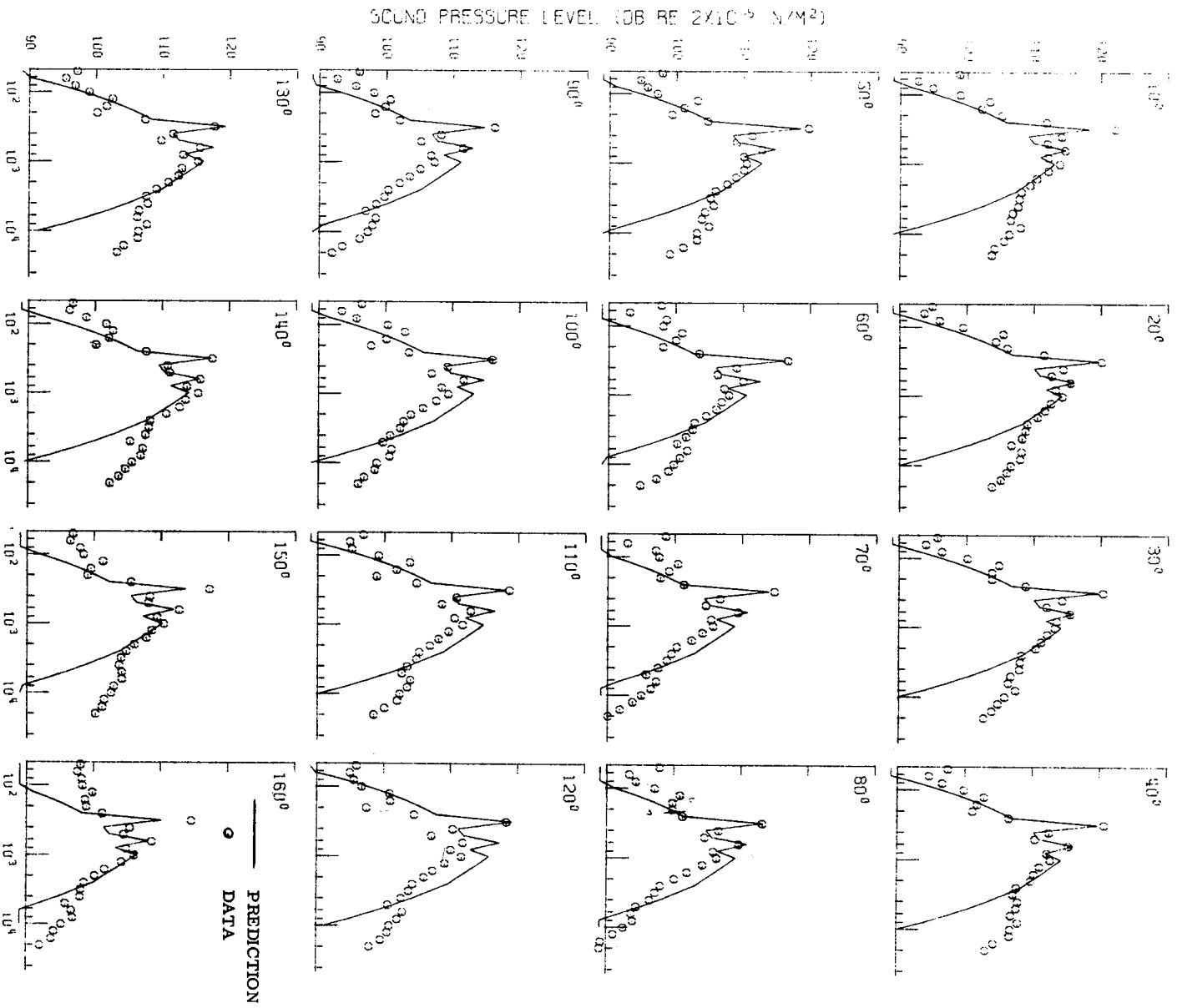
(aa) Fan QF-6, configuration 45, 80-percent speed.

Figure 19. - Continued.



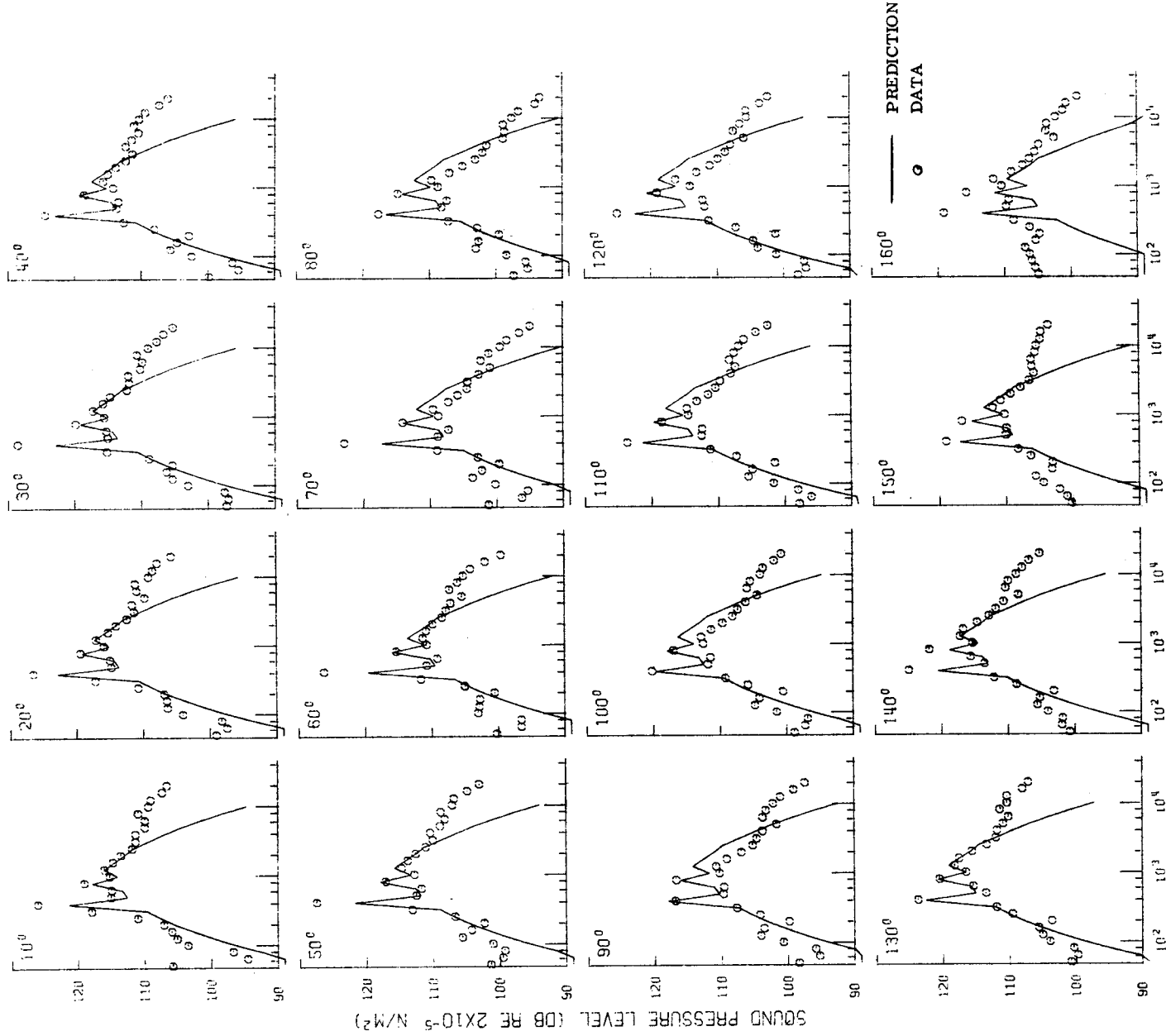
(bb) Fan QF-6, configuration 45, 90-percent speed.

Figure 19. - Continued.



(cc) Fan QF-9, configuration 51, 60-percent speed.

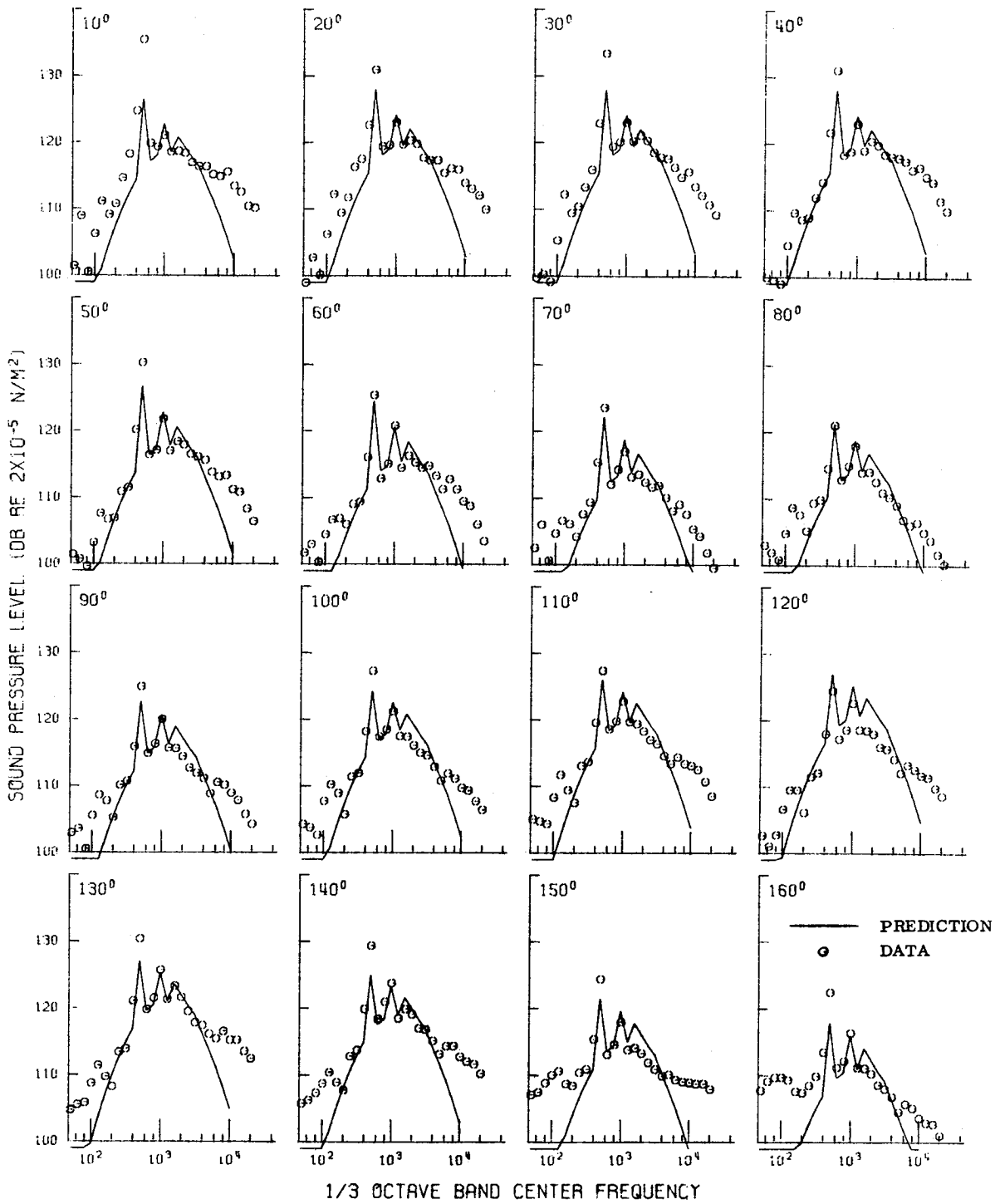
Figure 19. - Continued.



1/3 OCTAVE BAND CENTER FREQUENCY

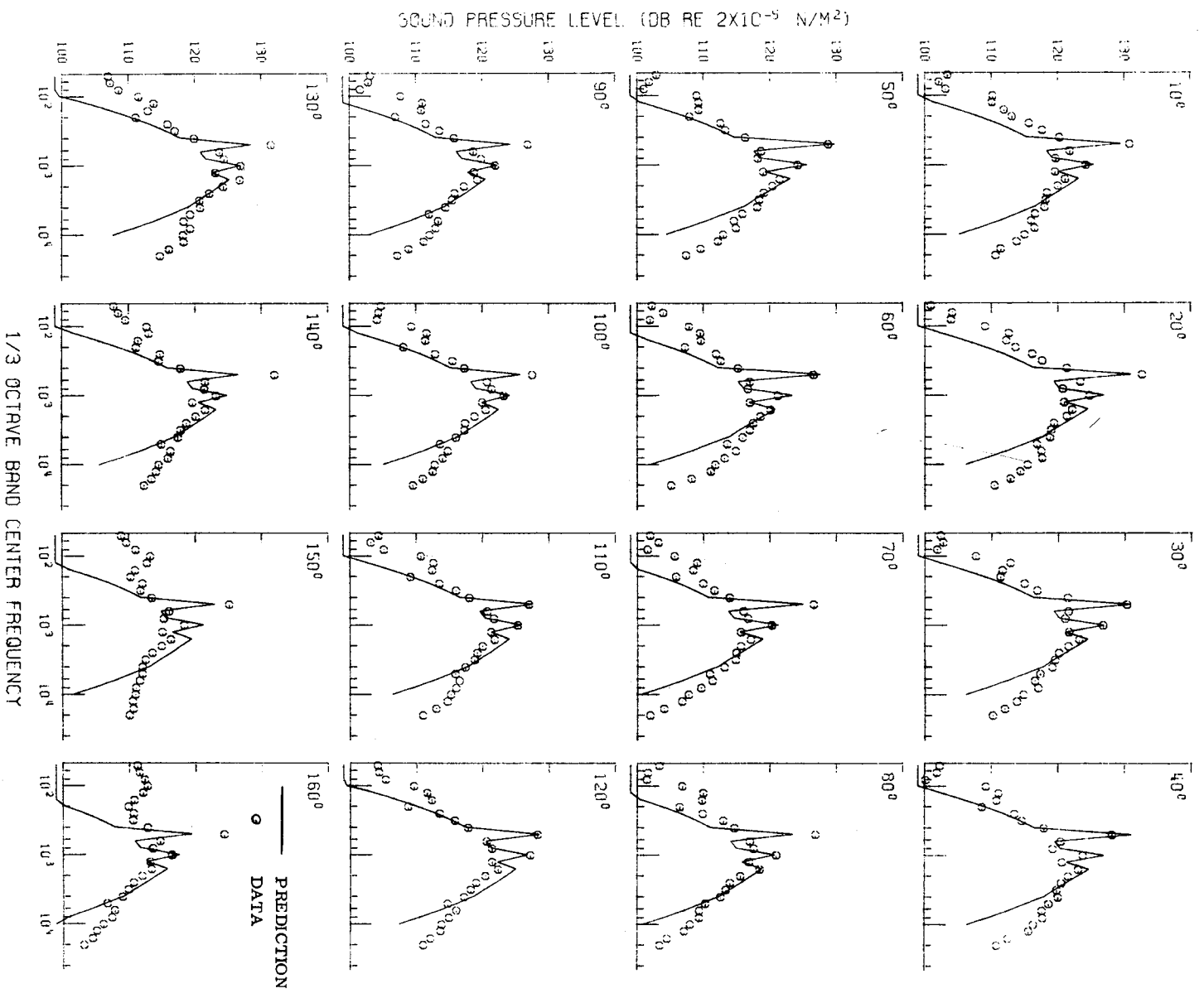
(dd) Fan QF-9, configuration 51, 70-percent speed.

Figure 19. - Continued.



(ee) Fan QF-9, configuration 51, 86-percent speed.

Figure 19. - Continued.



(H) Fan QF-9, configuration 51, 93-percent speed.

Figure 19. - Concluded.

1. Report No. NASA TM X-71763	2. Government Accession No.	3. Recipient's Catalog No.	
4. Title and Subtitle INTERIM PREDICTION METHOD FOR FAN AND COMPRESSOR SOURCE NOISE		5. Report Date June 1979	
		6. Performing Organization Code	
7. Author(s) Marcus F. Heidmann		8. Performing Organization Report No. E-8398	
		10. Work Unit No. 500-208	
9. Performing Organization Name and Address National Aeronautics and Space Administration Lewis Research Center Cleveland, Ohio 44135		11. Contract or Grant No.	
		13. Type of Report and Period Covered Technical Memorandum	
12. Sponsoring Agency Name and Address National Aeronautics and Space Administration Washington, D. C. 20546		14. Sponsoring Agency Code	
		15. Supplementary Notes First printing, 1975.	
16. Abstract A method is presented for interim use by NASA in assessing the noise generated by fans and compressors in turbojet and turbofan engines. One-third octave band sound pressure levels consisting of broadband, discrete-tone, and combination-tone noise components are predicted. Spectral distributions and directivity variations are specified. The method is based on that developed by other investigators with modifications derived from an analysis of NASA Lewis Research Center full-scale, single-stage fan data. Comparisons of predicted and measured noise performance are presented, and requirements for improving the method are discussed.			
17. Key Words (Suggested by Author(s)) Fan noise prediction method; Aircraft noise; Engine noise; Turbomachinery noise		18. Distribution Statement Unclassified - unlimited STAR Category 07	
19. Security Classif. (of this report) Unclassified	20. Security Classif. (of this page) Unclassified	21. No. of Pages 68	22. Price* A04